Leckie, R.M., Sigurdsson, H., Acton, G.D., and Draper, G. (Eds.), 2000
Proceedings of the Ocean Drilling Program, Scientific Results, Vol. 165

17. THE CARIBBEAN CARBONATE CRASH AT THE MIDDLE TO LATE MIOCENE TRANSITION: LINKAGE TO THE ESTABLISHMENT OF THE MODERN GLOBAL OCEAN CONVEYOR[1]

Joy M. Roth,[2,3] André W. Droxler,[2] and Koji Kameo[4]

ABSTRACT

Carbonate content and mass accumulation rate (MAR) were determined for Holes 998A, 999A, and 1000A recovered during the Ocean Drilling Program (ODP) Leg 165 in the Yucatan Basin (3101 m), the Colombian Basin (2839 m), and the Pedro Channel (927 m), respectively, for an interval spanning most of the middle Miocene and the early part of the late Miocene. Aragonite MAR was analyzed in Hole 1000A to detect dissolution of metastable carbonates at subthermocline depths in addition to sea-level variations. Oxygen and carbon stable isotope composition of benthic foraminifers are used as a proxy for sea-level fluctuations and as a record for the chemistry variations of deep and intermediate water, respectively. The middle to late Miocene transition in the Caribbean was characterized by massive increase of carbonate dissolution. Five well-defined dissolution episodes between 12 and 10 Ma are characterized by dramatic reductions in carbonate content and MAR. This interval is referred to as the Caribbean carbonate crash. The term "carbonate crash" was borrowed from ODP Leg 138 published results (Lyle et al., 1995). The timing and periodicity of four of the five carbonate-dissolution episodes in the Caribbean basins appear to correspond to the late middle Miocene production peaks of the North Component Water (Wright and Miller, 1996), equivalent to the modern North Atlantic Deep Water (NADW).

These findings suggest that the carbonate crash in the Caribbean and in the eastern equatorial Pacific was caused by a reorganization of the global thermohaline circulation induced by the re-establishment and intensification of the NADW production and concomitant influx of corrosive southern-sourced intermediate waters (analogous to the modern Antarctic Intermediate Water Mass) into the Caribbean. At the time of the late middle Miocene carbonate crash, the Caribbean became—and remains—an important pathway for the return flow of the global thermohaline oceanic circulation. Tectonic activity and foundering along the northern Nicaraguan Rise in the middle Miocene led to the establishment of a connection between the southern and northern Caribbean basins by the opening of two new main seaways, the Pedro Channel and the Walton Basin (Droxler et al., 1998). Once established, this connection triggered the initiation of the Caribbean/Loop Currents. The gradual closing of the Central American Seaway, simultaneous to the opening of seaways along the northern Nicaraguan Rise, disrupted the low latitude connection between the Atlantic and the eastern Pacific and, as a direct consequence, further strengthened the Caribbean Current. Based upon the observation of different coccolith assemblages present on either side of the Central American Seaway at some point during the middle to late Miocene transition, the Pacific-Atlantic connection might have been completely closed at that time. This full closure would explain the observed contemporaneous intermingling of terrestrial fauna between North and South America. The newly developed and strengthened Caribbean Current transported warm, saline waters of the Caribbean to the northern North Atlantic via the Loop Current, the Florida Current, and the Gulf Stream. These conditions were favorable for the contemporaneous re-establishment of NADW. This reorganization of the global oceanic circulation at the middle to late Miocene transition is well recorded in the contrasting carbonate preservation pattern observed in the Caribbean basins, the eastern equatorial Pacific, and the Ceara Rise (equatorial Atlantic).

INTRODUCTION

Dramatic reductions of calcium carbonate weight percent, lower calcium carbonate mass accumulation rates (MARs), and poorer preservation of calcium carbonate microfossils characterize the interval at the middle to late Miocene transition (12–10 Ma) in the Caribbean (Sigurdsson, Leckie, Acton, et al., 1997). This interval has been identified as the Caribbean "carbonate crash" at three Ocean Drilling Program (ODP) Leg 165 sites. Such significant changes in preservation of carbonate sediments are related to processes that affect the global carbonate and carbon budgets. Studying the nature, extent, and timing of these intense fluctuations in the burial of carbonate sediments should result in a better understanding of the changes in global thermohaline circulation and the establishment of the modern ocean circulation.

Similar occurrences of carbonate dissolution at the middle to late Miocene transition have been recorded previously in other parts of the world. Vincent (1981) reported unusually low carbonate weight percent at the Deep Sea Drilling Project (DSDP) Site 310 on the Hess Rise (north central Pacific) and referred to the interval as the mid-Epoch 10 event. Epoch 10 is now correlated with the 4a Chron interval spanning between 9.2 and 9.6 Ma, based upon the geomagnetic polarity time scale of Cande and Kent (1992). The interval between 11.2 and 8.6 Ma cored during ODP Leg 138 and other DSDP sites in the eastern equatorial Pacific is characterized by very low carbonate MARs (Fig. 1). This interval was referred to as the "carbonate crash" by Lyle et al. (1995) and was interpreted by these authors as a 1200-m shoaling of the lysocline. A long-term shoaling of the lysocline occurred in the middle Miocene from 14.0 to 11.5 Ma followed by a lysocline deepening at 10.5 Ma as recorded in several ODP Leg 154 sites drilled on the Ceara Rise in the western tropical Atlantic (King et al., 1997).

The comparable nature and partially overlapping timing of the carbonate reductions in the Pacific, Atlantic, and Caribbean suggest a common cause associated with changing oceanic circulation. The

[1]Leckie, R.M., Sigurdsson, H., Acton, G.D., and Draper, G. (Eds.), 2000. *Proc. ODP, Sci. Results,* 165: College Station, TX (Ocean Drilling Program).
[2]Department of Geology and Geophysics, Rice University, Houston, TX 77005-1892, U.S.A. Correspondence author: andre@rice.edu
[3]Texaco North American Production, P.O. Box 60252, New Orleans, LA 70160, U.S.A.
[4]Exploration Department, Teikoku Oil Company, Ltd. 1-31-10, Hatagaya, Tokyo, 151-8565, Japan.

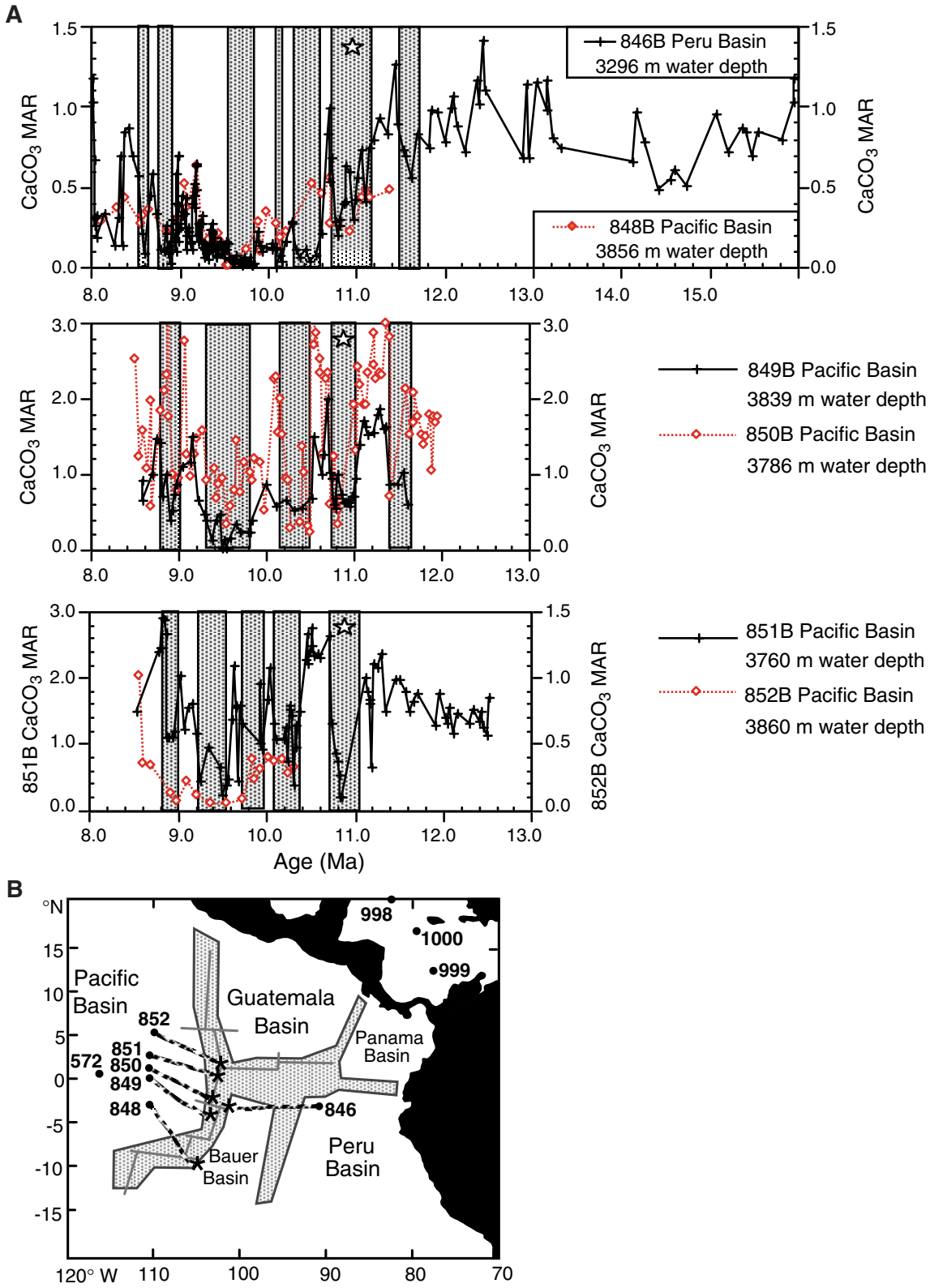

Figure 1. **A.** Carbonate mass accumulation rates (CO_3 MARs) for the eastern equatorial Pacific, ODP Leg 138, from Lyle et al. (1995). Shaded areas reflect intervals of carbonate dissolution. The first major dissolution interval in the eastern equatorial Pacific centered at 11 Ma is equivalent to Caribbean dissolution Episode III (see Figs. 9, 10), and is shown with an open star. **B.** Map of ODP sites in the eastern equatorial Pacific. Bullets mark current location and asterisks denote location backtracked to 10 Ma from Pisias, Mayer, Janecek, Palmer-Julson, and van Andel (1995).

opening and closing of gateways could have changed global ocean thermohaline circulation and, as a result, triggered the carbonate crash at the middle to late Miocene transition. Since the Cretaceous, the global ocean has evolved from a circum-tropical to circum-Antarctic surface circulation and from a halothermal to the thermohaline deep-water circulation of today (Kennett and Barker, 1990). The middle Miocene was a critical time of paleoceanographic reorganization during which time the oceanic circulation became more similar to that of today. Wright et al. (1992) and Wright and Miller (1996) place the initiation of a North Component Water (NCW), a precursor to the modern North Atlantic Deep Water (NADW) and a primary component of deep-water convection, in the late early Miocene. Other authors have suggested that the initial production of NADW occurred in the late middle Miocene. Woodruff and Savin (1989) proposed that NADW began approximately at 13.5 Ma (originally published ages translated to those of Raffi and Flores, 1995). More recently, Wei (1995) and Wei and Peleo-Alampay (1997) further constrained NADW initiation to 11.5 Ma. This age falls between the 13.2- and 10.4-Ma coccolith datums according to the biostratigraphy of Raffi and Flores (1995).

Two gateways within the Caribbean, the Central American Seaway and the Pedro Channel/Walton Basin on the northern Nicaraguan Rise, are thought to have been closing and opening, respectively, during the middle Miocene (Figs. 2–5) (Duque-Caro, 1990; Droxler et al., 1998, and references therein). Closure and opening of these gateways have initiated the Caribbean and Loop Currents, directly strengthened the Gulf Stream, triggered and/or re-established the NADW production, and, therefore, changed the global distribution of deep-water masses and affected the preservation of carbonate sediment in the major oceans.

The semi-enclosed nature of the Caribbean acts as a discriminating valve for inflowing water masses. The Caribbean's connection to the deep Atlantic Ocean is restricted by sills extending from Venezuela to the Greater Antilles. Today, the uppermost part of NADW (the upper NADW [UNADW]) can enter the Caribbean through the deepest sills, the Windward Passage at 1540 m and the Anegada-Jungfern Passage at 1800 m (Fig. 3). Antarctic Intermediate Water (AAIW) flows at depths of 800–1400 m, overriding the UNADW, and mixes with the UNADW upon entering the Caribbean just above sill depth (Fig. 6A) (Haddad, 1994; Haddad and Droxler, 1996). This mixture then fills the lower reaches of the Caribbean basins. The Caribbean physiography provides a unique setting where sediment at abyssal depths in the Caribbean basins is being influenced by water masses of intermediate origins (a mixture of AAIW and UNADW). The Caribbean ODP Sites 998, 999, and 1000 cover a range of paleodepths from abyssal to upper bathyal waters. Moreover, these three sites are also located on both sides of the northern Nicaraguan Rise (which contains the Pedro Channel) (Fig. 4) and are in the vicinity of the Central American Seaway (Fig. 3).

METHODS AND MATERIALS

Data Set

Three ODP sites drilled in the Caribbean during Leg 165 are used in this study. More than 350 m of core from the three sites was analyzed. Exact locations and water depths are listed for each site in Table 1 and illustrated in Figures 3 and 4. Samples measuring 10 cm^3 were collected approximately every 50 cm. Care was taken to avoid sampling within turbidites and ash layers. However, samples collected between ash layers can still consist of 5%–10% dispersed ash relative to the bulk sediment (Sigurdsson, Leckie, Acton, et al., 1997).

Site 998

Site 998, the northernmost site analyzed for this study, is located in a water depth of 3101 m in the Yucatan Basin on the northern flank of the Cayman Rise (Fig. 3). The sections sampled in interval 165-998A-15H-1, 21–23 cm, to 22X-6, 55–57 cm, (132.51–203.15 meters below seafloor [mbsf]) consist of nannofossil ooze with foraminifers and clays, clayey nannofossil mixed sediment interbedded with turbidites and ash layers, clays with nannofossils, nannofossil chalk with clays, and foraminifer chalk with clay (Sigurdsson, Leckie, Acton, et al., 1997). This 71-m-long section from Hole 998A corresponds to an early middle Miocene to late Miocene interval and contains ~32 turbidites adding up to 6.62 m of sediment (~9.5% of the total sediment) and 2.11 m of ash within 17 distinct layers (~3% of the total sediment).

Site 999

Site 999 is located on the Kogi Rise within the Colombian Basin (Fig. 3). The water depth of this site (2839 m) is almost a kilometer above the surrounding Colombian abyssal plain. It is the most proximal site to the Isthmus of Panama and also the closest to the mouth of the Magdalena River, an important source of fine terrigenous sediment. The 123-m-thick section of early middle to late Miocene-age sediment in Hole 999A (interval 165-999A-28X-1, 18–20 cm, to 38X-CC, 9–11 cm; 231.91–354.17 mbsf), consists of clayey nannofossil sediment with siliceous components, interbedded minor volcanic ash layers, clay with nannofossils, siliceous clayey mixed sediment, and clayey calcareous chalk with foraminifers and nannofossils (Sigurdsson, Leckie, Acton, et al., 1997). Samples below 300 mbsf are extremely indurated. In contrast to Site 998, no turbidites were observed in the middle to late Miocene core interval. Approximately 3.21 m of sediment (~3% of the total core) corresponding to 57 distinct ash layers was observed within this cored interval in Hole 999A (Sigurdsson, Leckie, Acton, et al., 1997).

Site 1000

The water depth of Site 1000, at 927 m, is the shallowest of the three sites included in this study (Figs. 3, 4). Located within the Pedro Channel, a seaway across the northern Nicaraguan Rise, Site 1000 is adjacent to active carbonate banks that export neritic, bank-derived carbonate sediment into the channel (Glaser and Droxler, 1993; Schwartz, 1996). The pelagic sediment is mixed with lateral influx of neritic carbonate and terrigenous sediments. The 172-m middle to late Miocene core interval of Hole 1000A consists of micritic nannofossil ooze with foraminifers, foraminiferal micritic ooze with nannofossils, and micritic nannofossil chalk with clay and foraminifers (Sigurdsson, Leckie, Acton, et al., 1997). The 0.99 m of combined ash layers and 1.21 m of turbidites (~0.5% and ~0.7% of the core interval, respectively) represent minor lithologies in this interval.

Stratigraphy

Age/depth models in this study are based on coccolith datums identified by Kameo and Bralower (Chap. 1, this volume). These models are based upon the biostratigraphy of Raffi and Flores (1995) (Fig. 7; Table 2). Figure 8B compares the planktonic foraminifer and nannofossil datums of the three sites. Hole 998A also includes the magnetostratigraphy of Shackleton et al. (1995), where the time scale is based upon astronomical tuning as well as gamma-ray attenuation porosity evaluator density correlation to further refine the work of Cande and Kent (1992). Good agreement between the nannofossil and foraminifer datums is observed. The nannofossil datums, however, suggest more uniform sedimentation rates. Sedimentation rate changes are calculated by linear interpolation between these datums (Fig. 8B).

Sample Processing and Analyses

Each sample was divided onto two aluminum weighing trays. The samples were then dried for at least 48 hr in an oven at 50°C. One portion was weighed, soaked in pH-balanced deionized distilled water,

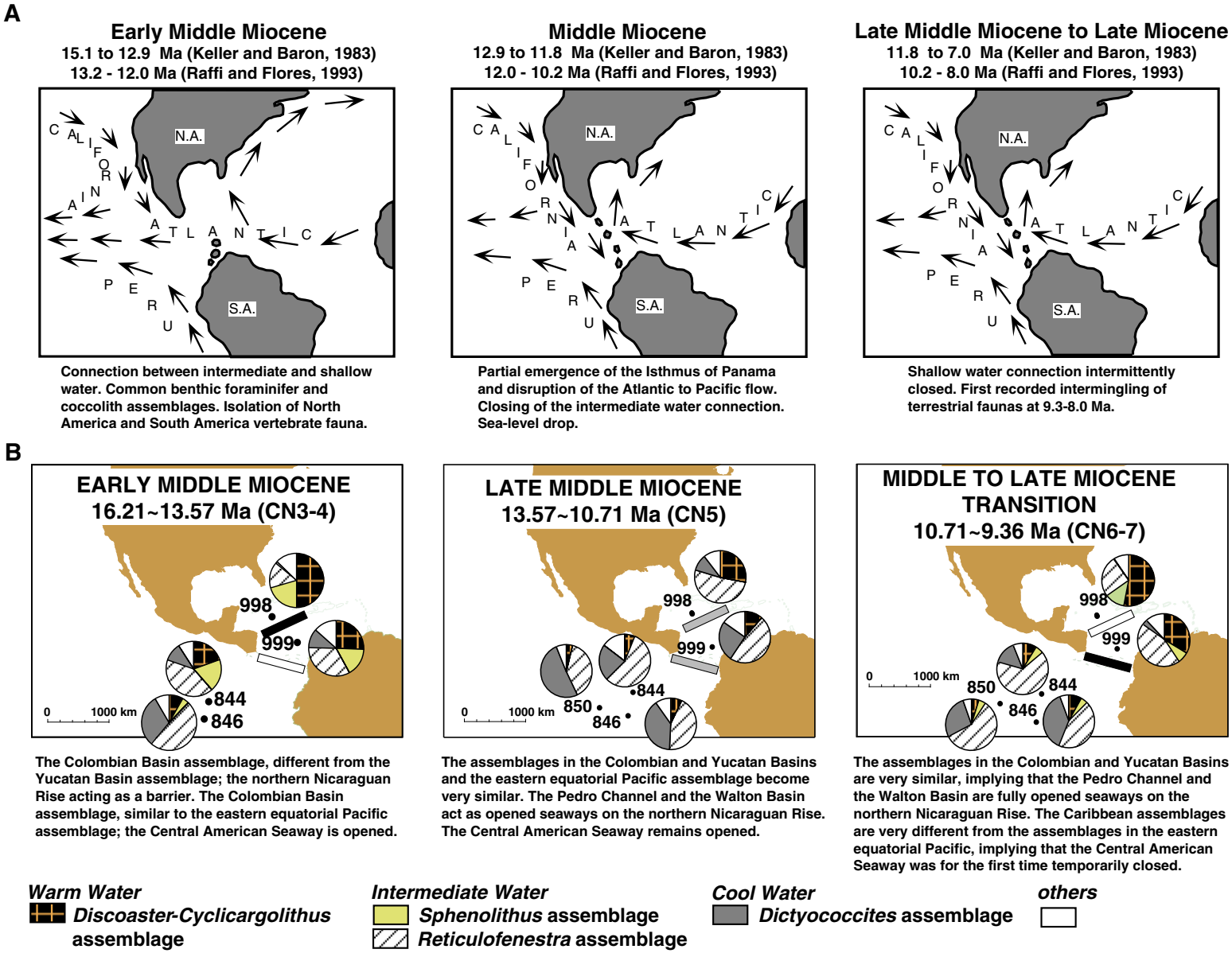

Figure 2. **A.** Tectonic and paleoceanographic evolution of the Central American Seaway with inferred surface circulation, modified from Duque-Caro (1990) and supplemented with data from Keller and Barron (1983), Vail and Hardenbol (1979), McDougall (1985), Webb (1985), Raffi and Flores (1995), and Kameo and Sato (in press). **B.** Middle to early late Miocene evolution of the coccolith assemblages in the southern (Colombian Basin) and northern (Yucatan Basin) Caribbean basins and the eastern equatorial Pacific with inferred status of gateway opening and closure on the northern Nicaraguan Rise and along the Central American arc (Kameo and Sato, in press). White rectangles = gateway open; gray rectangles = gateway partially open; black rectangles = gateway closed.

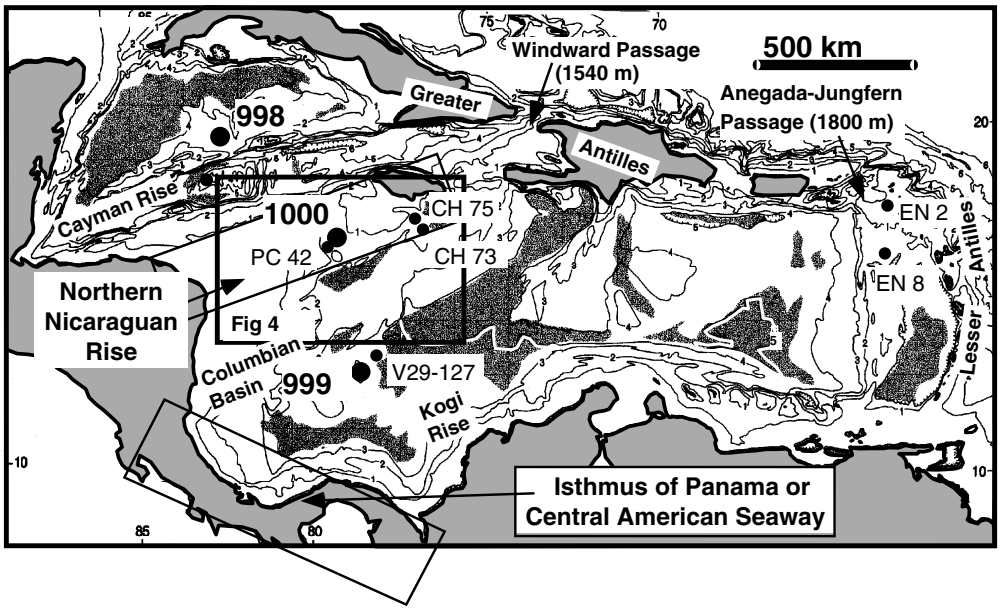

Figure 3. Map of the Caribbean showing the location of Caribbean ODP Sites 998, 999, and 1000 in relation to the two areas of the northern Nicaraguan Rise and the Isthmus of Panama that have played a critical role in the establishment of the modern ocean circulation. Tectonic activity has modified the bathymetry of these two areas. These modifications have influenced the general Atlantic circulation and, in particular, the southern/northern Caribbean and Atlantic/Pacific Ocean interchanges at various times during the middle and early late Miocene. CH = Cape Hatteras; V = Vema; EN = Endeavour.

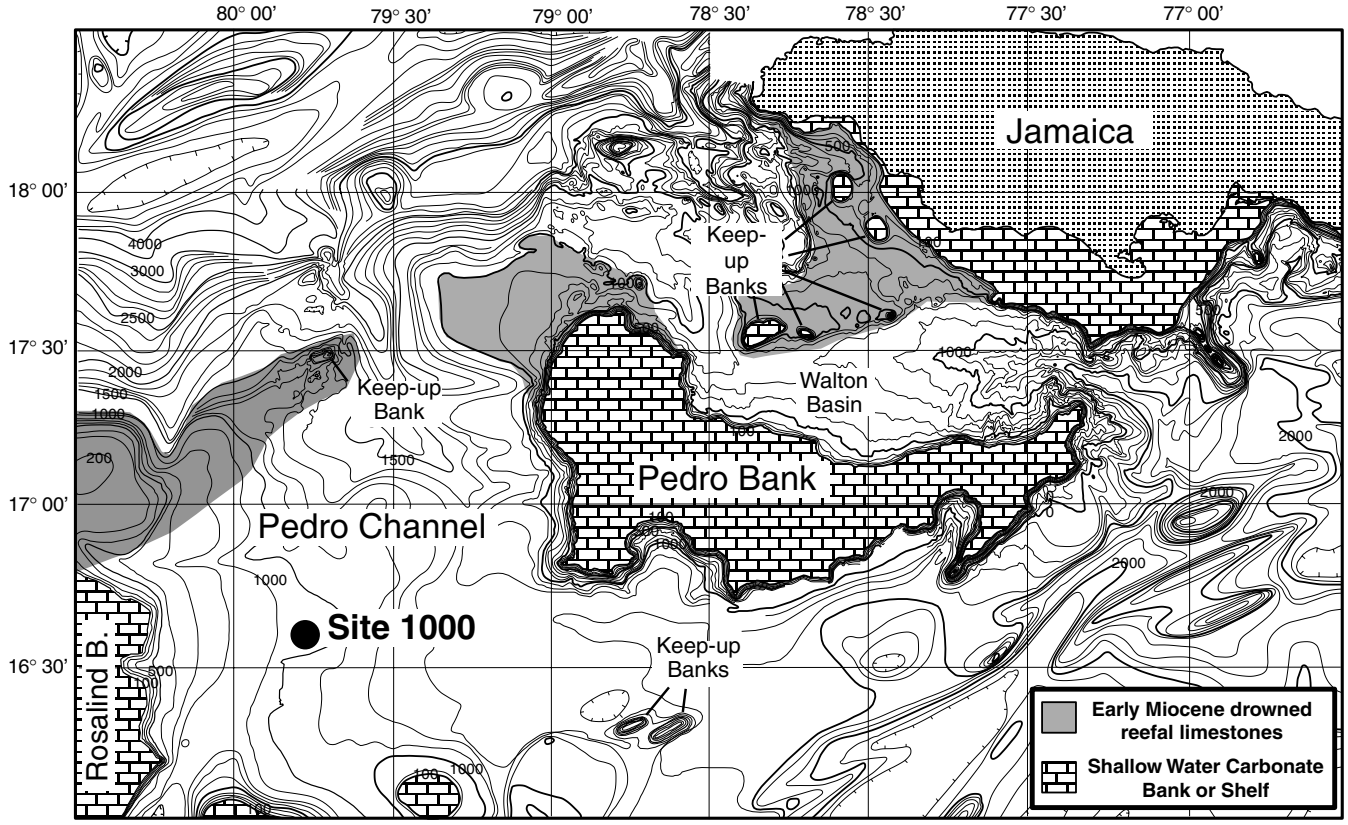

Figure 4. Detailed bathymetry in Pedro Channel and Walton Basin (Cunningham, 1998) represents the complexity and the segmented character of the seafloor morphology within the seaways along the northern Nicaraguan Rise. In association with the present-day carbonate banks (brick pattern) that have remained areas of neritic carbonate since the late Eocene, drowned banks and reefs observed in Pedro Channel and Walton Basin formed an east-west barrier along the northern Nicaraguan Rise, where continuous shallow-water environments prevailed from the late Eocene to early Miocene. Some of the carbonate banks and barriers (light gray pattern) subsided and drowned as late as the late middle Miocene (Cunningham, 1998). ODP Site 1000 is located in the Pedro Channel.

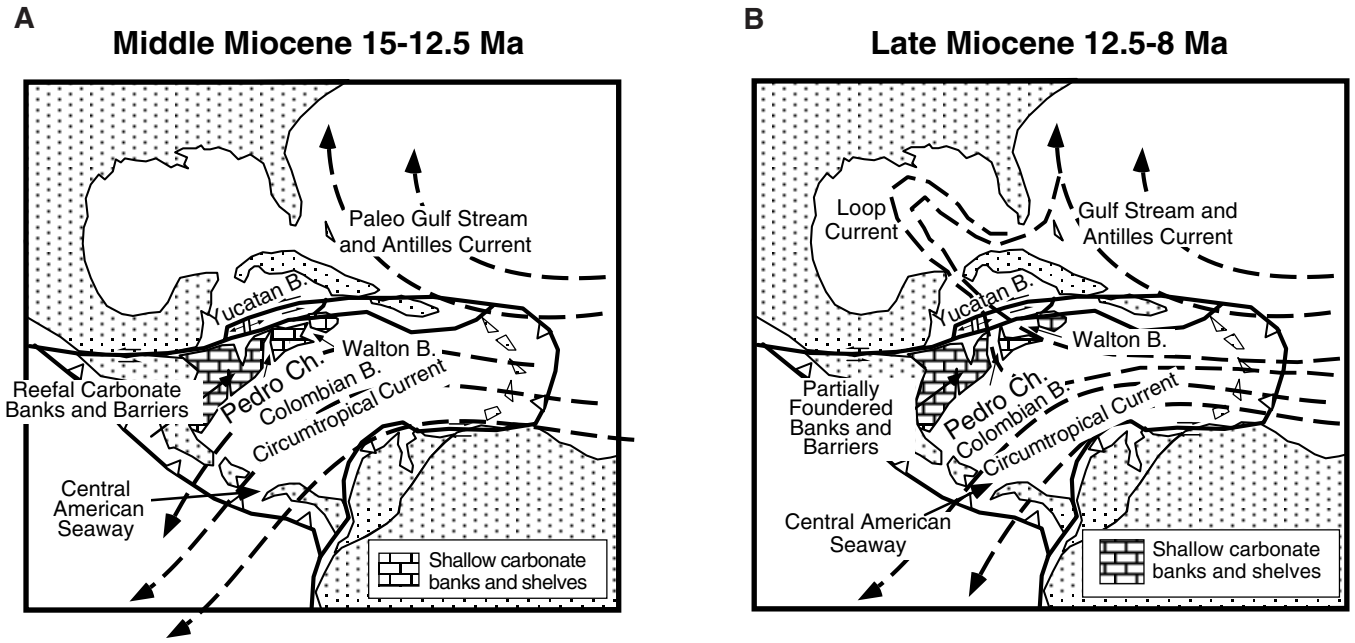

Figure 5. Simplified reconstruction sketches of the Caribbean (after Pindell, 1994) illustrating several scenarios for closure and opening of gateways in the Caribbean. **A.** Scenario in the early middle Miocene, when nearly continuous carbonate banks and barrier reefs isolated the southern from the northern Caribbean basins, enhanced the water exchange between the eastern Pacific and the western tropical Atlantic, and minimized the development of a western boundary current within the Caribbean. **B.** Scenario at the middle to late Miocene transition, when the partial foundering and subsidence of the continuous shallow carbonate system along the northern Nicaraguan Rise opened the connection between the southern and the northern Caribbean basins; the Caribbean/Loop Currents were established as the consequence of this partial collapse. The establishment of the Caribbean/Loop Currents strengthened the Gulf Stream. A stronger western boundary current can explain the contemporaneous re-establishment of a strong North Component Deep Water in the high latitudes of the North Atlantic (Wright and Miller, 1996) that triggered a global ocean conveyor belt similar to the one we know today. This scenario can explain the carbonate crash on both sides of the Isthmus of Panama (see "Caribbean Gateways, Establishment of the Caribbean Current, and NADW Production," this chapter).

and sieved through a 63-µm screen. The coarse (sand sized) fraction was then dried and reweighed for relative proportions of the coarse fraction to the bulk sediment. Indurated samples were also soaked in a sodium hexametaphosphate solution to aid in disaggregation.

Stable Isotopes

The sand-sized particles were dry sieved through a 250-µm screen and picked for the benthic foraminifer *Planulina wuellerstorfi,* which records oxygen and carbon isotopes of the ambient waters (Shackleton and Opdyke, 1973; Belanger et al., 1981). Relative preservation of the benthic tests, such as the degree of cementation, was also recorded. The *P. wuellerstorfi* tests were cleaned by sonication in deionized, distilled water and analyzed in Dr. Howard Spero's stable isotope laboratory at the University of California-Davis. The foraminifers were reacted in a common phosphoric acid bath fed by an autocarbonate device and analyzed in a Fisons Optima mass spectrometer. Values for the mass ratios of $^{18}O/^{16}O$ and $^{13}C/^{12}C$ were related to the Peedee belemnite standard and reported as $\delta^{18}O$ and $\delta^{13}C$, respectively, with a precision of 0.08‰ for $\delta^{18}O$ and 0.05‰ for $\delta^{13}C$.

Carbonate Content

The second portion of bulk sediment was ground with a mortar and pestle. Half-gram portions of the powder were analyzed in a carbonate bomb for carbonate content (Müller and Gastner, 1971). Within the sealed cylinder, 50% concentrated HCl was reacted with the sample. The increased pressure from the generated carbon dioxide is proportional to the initial amount of carbonate (Droxler et al., 1988) when compared to a 100% pure calcium carbonate standard. The carbonate weight percent was derived using the following equation:

$CaCO_3$ wt% = [(sample pressure/sample weight) / (standard pressure/standard weight)] × 100.

Standards are run at the beginning and end of a batch of 10 unknowns to ensure consistency. These are the same procedures described in Glaser and Droxler (1993). Carbonate data acquired in the Rice University lab using this procedure were integrated with Leg 165 shipboard data. Inorganic geochemical analyses were conducted during ODP Leg 165 on one sample per section of core (approximately every 150 cm). Carbonate weight percent was obtained on the ship by reacting 10 mg of dried, ground, bulk sample with HCl in a Coulometrics 5011 coulometer (for methods, see the "Explanatory Notes" chapter in Sigurdsson, Leckie, Acton, et al., 1997). No discrepancy between the two methods was observed in the carbonate analysis (Fig. 9). The resolution of the carbonate records was certainly improved by merging both shipboard and postcruise carbonate data sets for Sites 998, 999, and 1000.

Mass Accumulation Rates

Accumulation rates of the bulk sediment are calculated by multiplying a linear sedimentation rate (in meters per million years) by the dry bulk density (grams of dry sediment per wet volume in cubic centimeters):

Dry bulk density × linear sedimentation rate = bulk MAR.

Carbonate MARs (CO_3 MARs) are calculated by multiplying the MAR by the calcium carbonate content:

MAR × $CaCO_3$ wt% × 100 = CO_3 MAR.

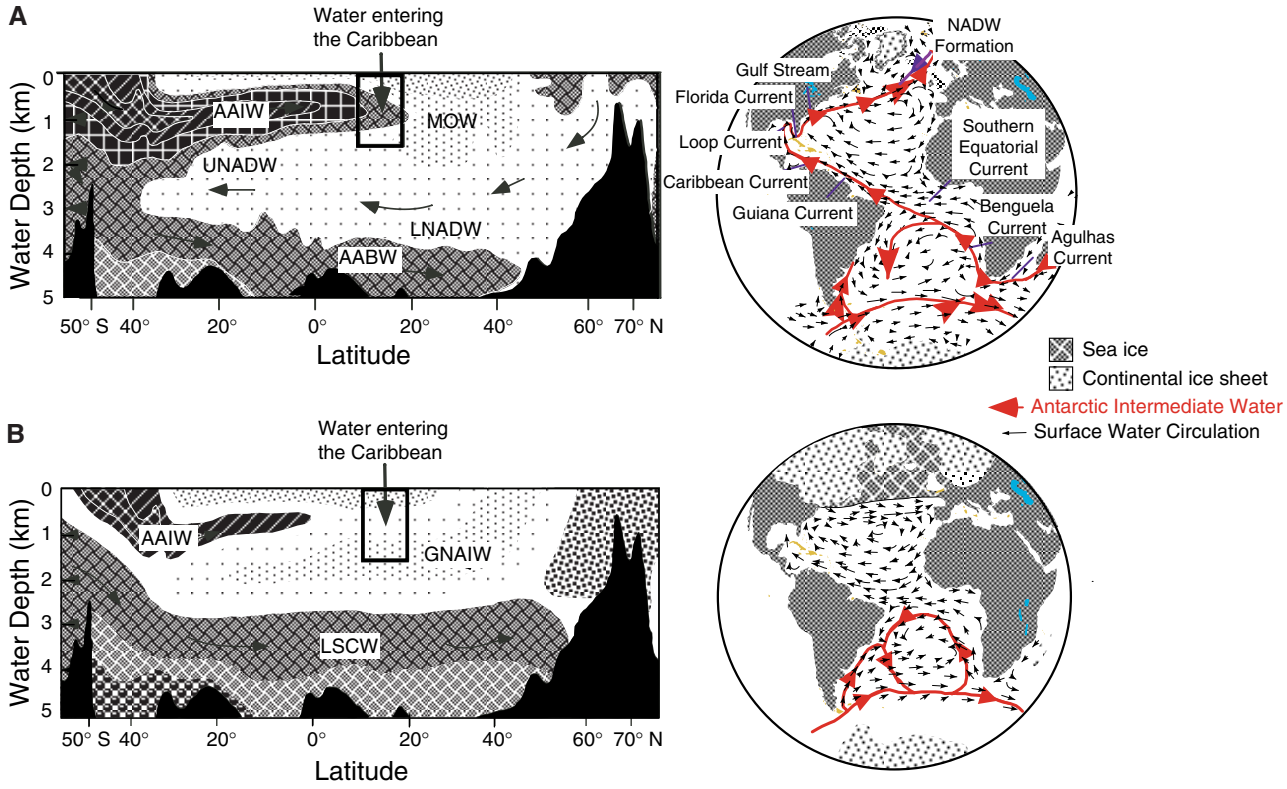

Figure 6. **A.** Circulation of water masses along a north-south profile of the modern Atlantic Ocean. Atlantic surface and Antarctic Intermediate Water circulation are also shown on a map view (Gordon, 1986; modified by Haddad and Droxler, 1996). AABW = Antarctic Bottom Water; AAIW = Antarctic Intermediate Water; LNADW = lower North Atlantic Deep Water; UNADW = upper North Atlantic Deep Water; MOW = Mediterranean Outflow Water. **B.** Postulated circulation of water masses along a north-south profile of the Atlantic Ocean during the last glacial maximum (LGM). Inferred surface and intermediate water circulation during the LGM are also shown on a map view. GNAIW = glacial North Atlantic Intermediate Water. Figures also schematically show the water at latitudes and depths to enter the Caribbean over sills in the Antilles. From Haddad and Droxler (1996).

Table 1. Location, coordinates, and water depth of the cores.

Hole	Location	Latitude	Longitude	Water Depth (mbsl)
998A	Cayman Rise, Yucatan Basin	19°29.377′N	82°56.166′W	3179.9
999A	Koji Rise, Colombian Basin	12°14.639′N	78°44.360′W	2827.9
1000A	Pedro Channel, Northern Nicaraguan Rise	16°33.223′N	79°52.044′W	915.9

The dry bulk density was directly measured from each core section as routine shipboard analysis during Leg 165. The sedimentation rate was calculated using the biostratigraphic datums of Raffi and Flores (1995) (Figs. 7, 8). CO_3 MAR, as opposed to carbonate weight percent, reflects what is happening to the carbonate only, rather than how the carbonate changes relative to other constituents. Despite being derived from other measurements, the calculation of MAR can be extremely helpful in discerning changes because of dissolution of carbonates and dilution by noncarbonates.

Carbonate Mineralogy

Because of its location in relatively shallow depths and its proximity to carbonate banks, the ground bulk sediment of Hole 1000A was also used to acquire mineralogical data of two carbonate species present in the core. A Philips-Norelco model 12045 X-ray diffractometer was used to scan the 2-θ angles from 25.5° to 27.5° and from 28.5° to 32° at a resolution of 0.02° per step. The area above the background radiation and under the aragonite peak (d-spacing = 3.41) and calcite peak (d-spacing = 3.04) was integrated. Greater description of this procedure and its quantitative range can be found in Milliman (1974) and Droxler et al. (1988). Because the aragonite content was reported as a percentage of the total carbonate, an aragonite accumulation rate was calculated by multiplying the aragonite content by the CO_3 MAR.

RESULTS

Age Models

The absolute timing and assigned ages of biostratigraphic datums often change with the refinement of successive chronostratigraphic studies. In the past decade or so, biostratigraphers have assigned significantly different ages with differences of as much as 2 m.y. to the same biostratigraphic datum (Fig. 7). It is, therefore, imperative to either identify the biostratigraphic time scale used when referring to ages of different age models or simply refer to the biostratigraphic zone within which an event lies. Fortuitously, the biostratigraphic datums of Raffi and Flores (1995) were also used in the age models for ODP Legs 138 and 154, placing their ages in a common biostratigraphic time frame with that of Leg 165. After establishing that the coccolith datums were reliable and corroborated by the magnetostratigraphy and foraminiferal datums, age models were generated for each site (Sites 998, 999, and 1000) (Fig. 8). The depth and calculated age are displayed in Figure 8B for every sample analyzed in this study.

Despite numerous turbidites observed in Hole 998A on the Cayman Rise (Yucatan Basin), the sedimentation rate for the middle to upper Miocene segment in Hole 998A is very linear with essentially

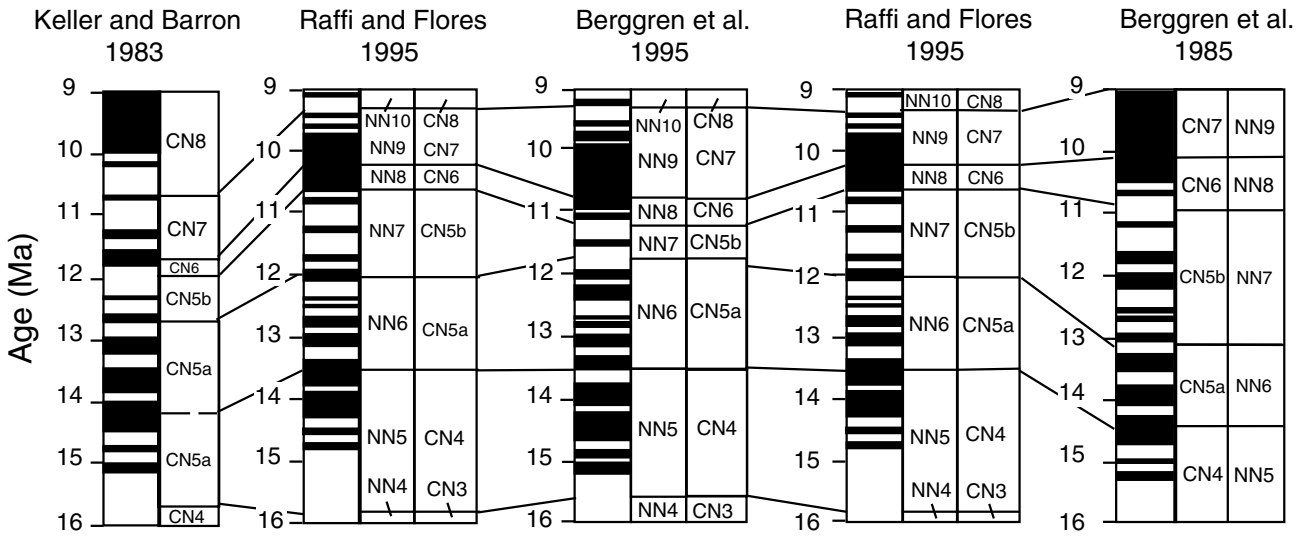

Figure 7. Biostratigraphies and associated magnetochronologies referred to in this study as compared to that of Raffi and Flores (1995). Note how particular nannofossil zones can vary by 2 m.y.

Table 2. Leg 165 datums for nannostratigraphy, planktonic foraminiferal stratigraphy, and magnetostratigraphy.

	Age (Ma)	Datum (mbsf)	Zone/Chron (base)	Nannozone (base)	Species	Reference
Hole 998A						
Nannostratigraphy	8.35	126.4	CN9a	NN11	FO *Discoaster berggrenii*	Raffi and Flores (1995)
	9.36	136.65	CN8a	NN10	LO *Discoaster hamatus*	Raffi and Flores (1995)
	10.39	149.15	CN7	NN9	FO *Discoaster hamatus*	Raffi and Flores (1995)
	10.71	151.4	CN6	NN8	FO *Catinaster coalitus*	Raffi and Flores (1995)
	11.74	157.9	CN5b	NN7	B acme *Discoaster kugleri*	Raffi and Flores (1995)
	13.19	171.3			T *Cyclicargolithus floridanus*	Raffi and Flores (1995)
	13.57	172.7	CN5a	NN6	T *Sphenolithus heteromorphus*	Raffi and Flores (1995)
	16.21	200.55			T acme *Discoaster deflandrei*	Raffi and Flores (1995)
Planktonic foraminiferal	8.2	142.21	N17		FO *Globorotalia plesiotumida*	Curry et al. (1995)
stratigraphy	10.3	148.99	N15		LO *Paragloborotalia mayeri*	Curry et al. (1995)
	11.8	161.03	N13		LO *Fohsella fohsi* s.l.	Berggren et al. (1995)
	12.7	187.94	N12		FO *Fohsella fohsi* s.l.	Berggren et al. (1995)
	14	208.21	N11		FO *Fohsella praefohsi*	Curry et al. (1995)
	14.8	208.21	N10		FO *Fohsella peripheroacuta*	Berggren et al. (1995)
Magnetostratigraphy	8.631	136.4	C4An (t)			Shackleton et al. (1995)
	8.945	137.3	C4An (o)			Shackleton et al. (1995)
	9.639	141.5	C5n (t)			Shackleton et al. (1995)
	10.839	156.63	C5n (o)			Shackleton et al. (1995)
	11.841	159.33	C5An (t)			Shackleton et al. (1995)
	12.32	166.95	C5An (o)			Shackleton et al. (1995)
	12.929	169.65	C5AAn (t)			Shackleton et al. (1995)
	13.083	173.1	C5AAn (o)			Shackleton et al. (1995)
	13.666	174	C5ACn (t)			Shackleton et al. (1995)
	14.053	175.05	C5ACn (o)			Shackleton et al. (1995)
	14.159	176.35	C5ADn (t)			Shackleton et al. (1995)
	14.607	179.2	C5ADn (o)			Shackleton et al. (1995)
	16.014	203.5	C5Cn (t)			Shackleton et al. (1995)
Hole 1000A						
Nannostratigraphy	8.35	286.05	CN9a	NN11	FO *Discoaster berggrenii*	Raffi and Flores (1995)
	9.36	331.3	CN8a	NN10	LO *Discoaster hamatus*	Raffi and Flores (1995)
	10.39	369.7	CN7	NN9	FO *Discoaster hamatus*	Raffi and Flores (1995)
	10.71	377.25	CN6	NN8	FO *Catinaster coalitus*	Raffi and Flores (1995)
	11.74	428.55	CN5b	NN7	B acme *Discoaster kugleri*	Raffi and Flores (1995)
	13.19	498.35			T *Cyclicargolithus floridanus*	Raffi and Flores (1995)
	13.57	514	CN5a	NN6	T *Sphenolithus heteromorphus*	Raffi and Flores (1995)
Planktonic foraminiferal	8.2	327.3	N17		FO *Globorotalia plesiotumida*	Curry et al. (1995)
stratigraphy	10	356.3	N16		FO *Neogloboquadrina acostaensis*	Curry et al. (1995)
	10.3	365.7	N15		LO *Paragloborotalia mayeri*	Curry et al. (1995)
	11.4	384.9	N14		FO *Globoturborotalita nepenthes*	Curry et al. (1995)
	11.8	394.55	N13		LO *Fohsella fohsi* s.l.	Berggren et al. (1995)
	12.3	423.45			FO *Globorotalia lenguaensis*	Curry et al. (1995)
	12.7	471.5	N12		FO *Fohsella fohsi* s.l.	Berggren et al. (1995)
	14	510	N11		FO *Fohsella praefohsi*	Curry et al. (1995)

Note: FO = first occurrence; LO = last occurrence; B = bottom; T = top; (t) = termination; (o) = onset.

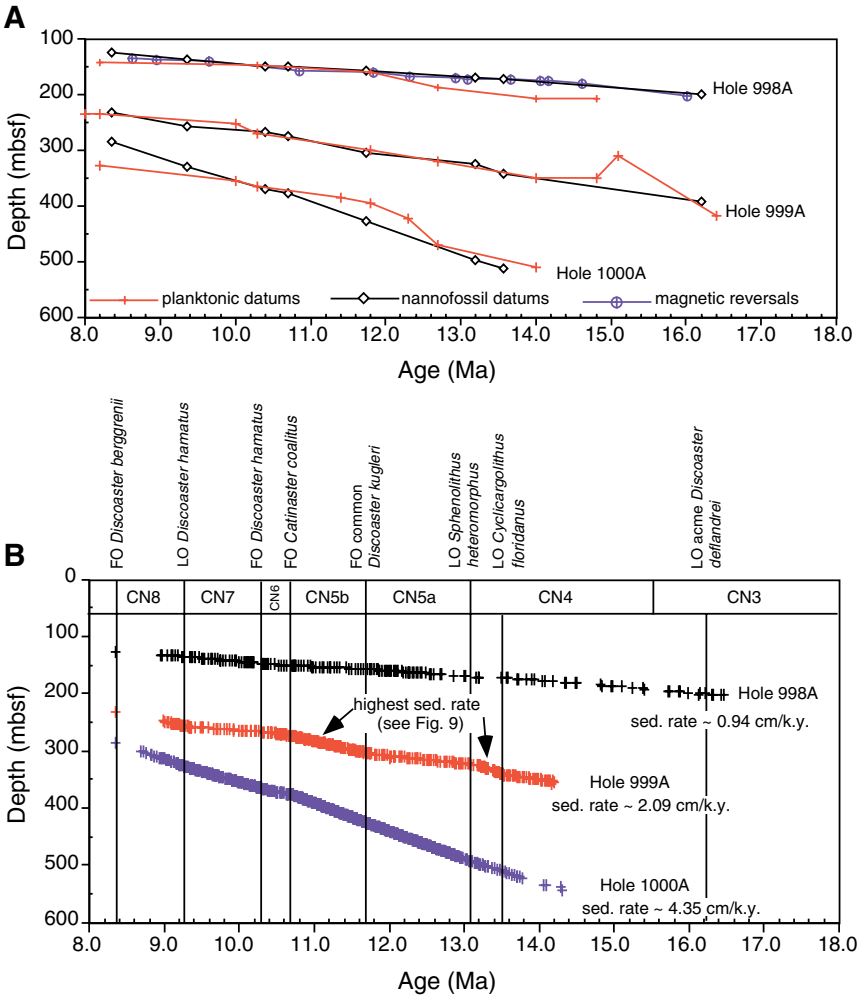

Figure 8. **A.** Shipboard datums of planktonic foraminifers, nannofossils, and magnetic reversals (Sigurdsson, Leckie, Acton, et al., 1997). **B.** Age model used in this study based on nannofossil datums only. Each hachure represents the age/depth relationship for a sample from this study; every sample of this study is represented.

a constant sedimentation rate of 0.94 cm/k.y. (Fig. 8B). Based upon this sedimentation rate, the lowest among the three studied Caribbean sites, the 50-cm-spaced samples correspond to a temporal resolution of ~53,000 yr.

The average sedimentation rate in the section of Hole 999A on Kogi Rise (Colombian Basin) is not as linear as Site 998 and shows the most variation of the three sites. Although the average rate is 2.09 cm/k.y., the sedimentation rates range from a low of 0.9 cm/k.y. (10.39–9.36 Ma) to 4.5 cm/k.y. (13.57–13.19 Ma) (Fig. 8B). The observed variability can be attributed to variable siliciclastic input at Site 999 because of the relative proximity of the Magdalena River mouth on the northern coast of Colombia. Because of a higher sedimentation rate in Hole 999A, the 50-cm-spaced samples in this study yield on average a temporal resolution of ~24,000 yr.

Among the three locations, the highest average sedimentation rate (4.35 cm/k.y.) is observed from ~13.3 to 10.7 Ma in Hole 1000A (Fig. 8B). This high sedimentation rate is likely related to the bank-derived neritic component added to the pelagic carbonates. This average sedimentation rate yields an average temporal resolution of 12,000 yr for the 50-cm-spaced samples of this study. As in Hole 998A, the sedimentation rate remains relatively constant. However, during Zone CN6 (10.39–10.71 Ma), the sedimentation rate was only 2.4 cm/k.y., about half the average rate observed for the middle to upper Miocene in Hole 1000A. Though Hole 998A displays the lowest resolution of the three sites, the samples available in that hole extend to 16 Ma as opposed to 14 and 13.8 Ma for Holes 999A and 1000A, respectively.

Coarse Fraction

Extensive induration of the lower reaches of Hole 999A prevented complete disaggregation and determination of the coarse fraction, and for similar reasons, no coarse-fraction data exists for Hole 1000A. In samples that could be disaggregated and sieved, comparing the mass ratio of the sand-sized fraction to the bulk sample is used as a proxy for reduced carbonate preservation (Berger, 1970b; Bassinot et al., 1994, and references therein). Because foraminiferal calcium carbonate tests become fragmented with dissolution, the coarse-fraction weight percent of a given sample is expected to give some indication of its degree of preservation (i.e., decreasing sand content with increasing dissolution).

Most of the coarse-fraction data from Hole 998A varies within a narrow range (0.2%–3.5%); occasionally it exceeds 10% at the beginning and end of the record (Fig. 10A). Times of reduced coarse sediment occur as both short intervals and distinct low points. The coarse-fraction percent remains generally low from 13.6 to 9.5 Ma. A relative preservation index, assigned to Hole 998A planktonic foraminifers during the cruise, reveals a significant decrease in preservation between 150 and 160 mbsf (~10.5–12.0 Ma), bracketing the interval of the carbonate crash. At 9.5 Ma, the coarse-fraction percent quickly increases to a level similar to that prior to 14 Ma. Observations for the interval between 16.4 and 13.8 Ma are not as well supported by the data because of the low sample resolution (200–400 k.y.).

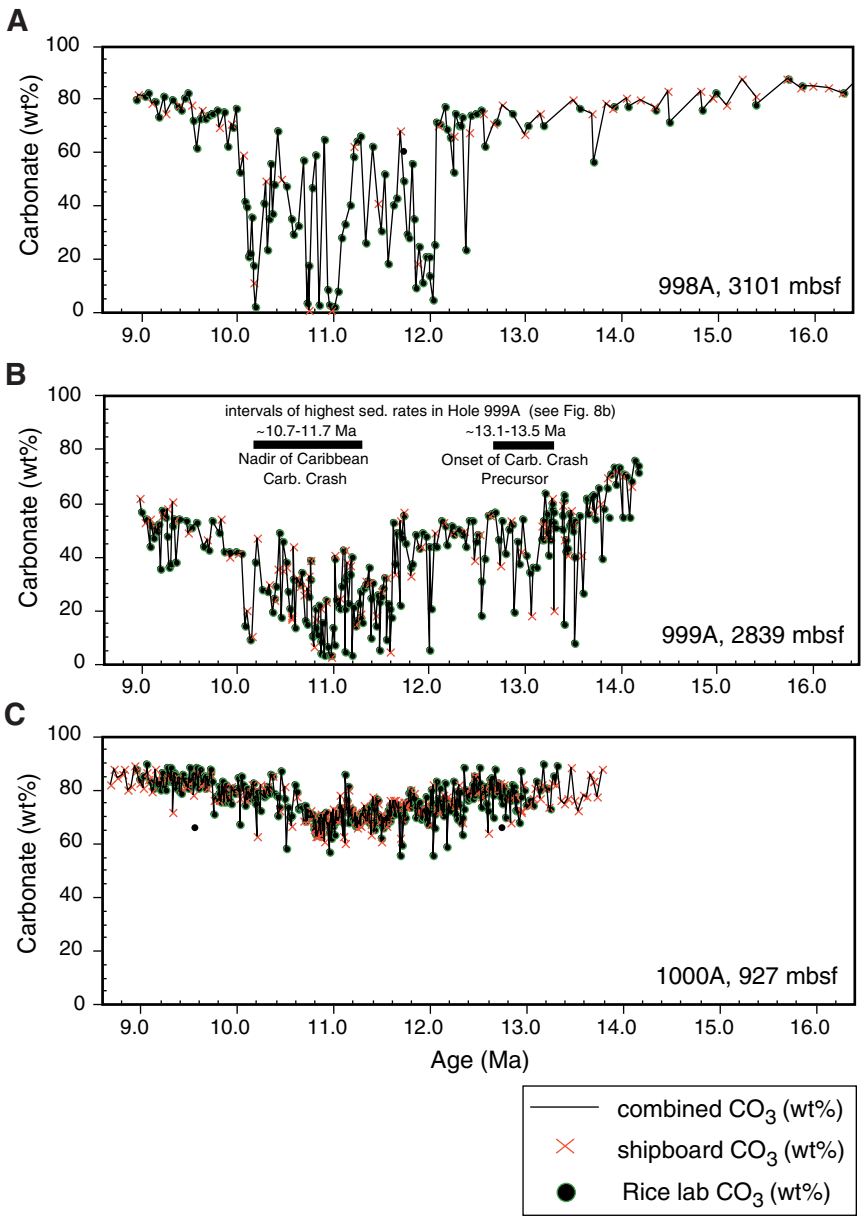

Figure 9. Comparison of two carbonate-content data sets derived from Leg 165 shipboard analyses and post-cruise Rice University analyses. **A.** Hole 998A. **B.** Hole 999A. **C.** Hole 1000A. Note that the carbonate 0–100 wt% range of the vertical axes is at the same scale for the three plots.

Coarse-fraction percent for Hole 999A is limited to an interval between 11.55 and 9.0 Ma (Fig. 10B). In this time span, a series of seven intervals characterized by a low coarse-fraction percent (<2%) was observed (Fig. 10B). The timing of these intervals generally corresponds to times of low coarse-fraction values in Hole 998A (Fig. 10A).

Carbonate Content

Reduction in the calcium carbonate weight percent is seen in the three sites (Figs. 9, 11). The carbonate content reflects proportional changes in the amount of carbonate and noncarbonate sediments. The greatest carbonate reductions are observed in Holes 998 and 999 during an interval between ~12.1 and 9.8 Ma, and referred to as the Caribbean carbonate crash. Hole 998A, drilled at 3101 m water depth and, therefore, the deepest site in this study, displays the largest amplitudes (0–80 wt%) in the carbonate-content variation. Prior to the Caribbean carbonate crash, carbonate-content values averaged ~80 wt% in Hole 998A (Fig. 9A). During the carbonate crash, carbonate-content values display several high-amplitude fluctuations. Eight samples within the carbonate-crash interval contain <5 wt% carbonate. Carbonate content returns to pre-carbonate-crash levels by 10 Ma.

Hole 999A, drilled at the slightly shallower depth of 2839 meters below sea level (mbsl), has carbonate-content reductions of a comparable scale to those in Hole 998A. Carbonate of the samples averages ~75 wt% before the carbonate crash, decreases to <5 wt% during the crash interval, and increases to 62 wt% by 9 Ma (Fig. 9B).

The carbonate content of Hole 1000A displays smaller variations than Sites 998 and 999 through the middle to upper Miocene transition. The carbonate is >80 wt% before the crash, decreases below 70 wt% during the crash, and recovers above 80 wt% after the crash (Fig. 9C). Although the magnitude of the change is not on the same scale as that of Sites 998 and 999, the 30 wt% decrease is significant because the water depth of Site 1000 is shallower than the modern calcite lysocline.

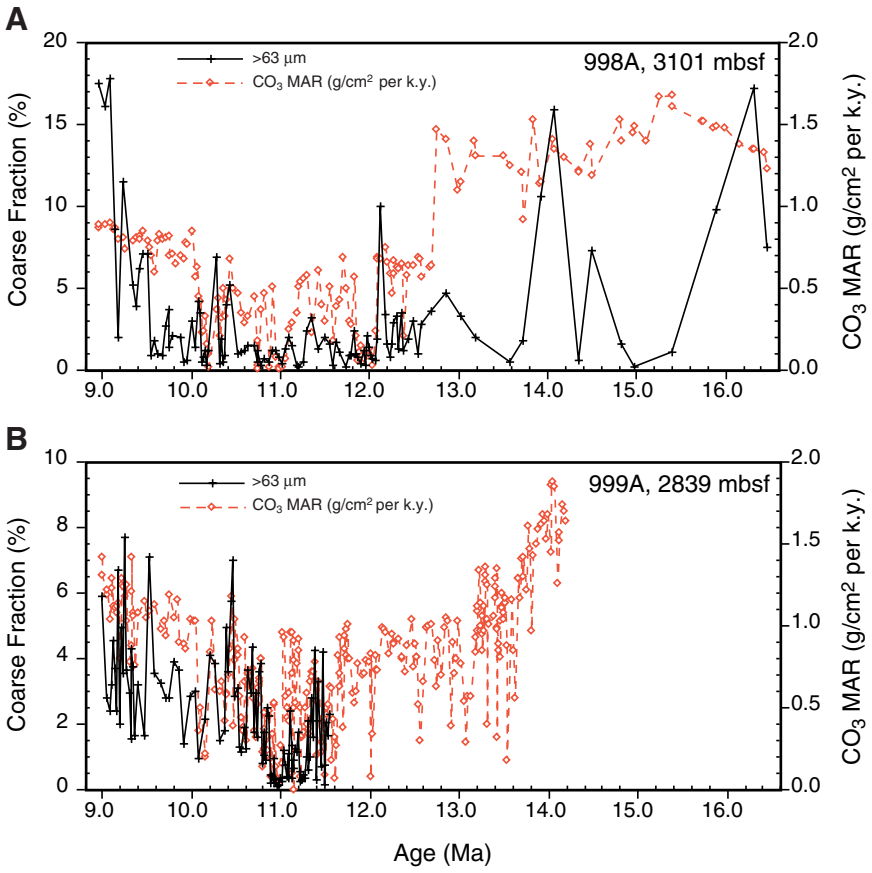

Figure 10. Sand-sized fraction, a proxy for carbonate dissolution, compared to carbonate mass accumulation rates (CO_3 MARs). **A.** Hole 998A. **B.** Hole 999A.

Figure 11 shows carbonate contents scaled to the range exhibited in each site. It is clear that the timing of intervals characterized by dramatic or significant carbonate reduction is remarkably similar at all three sites (Fig. 11). Carbonate weight percent in Hole 998A shows a very gradual 10% decrease from 16.4 to 12.4 Ma prior to the carbonate-crash interval. Then high-amplitude swings of carbonate values are encountered during a period initiated at ~12.1 Ma. During an interval lasting 1.9 Ma, carbonate values switch five times between 5 and 65 wt%. The incidents of minimum carbonate weight percent occur at 12.0–11.8, 11.6–11.4, 11.0–10.8, 10.6–10.5, and 10.3–10.1 Ma. These five episodes, characterized by carbonate minimum values within the Caribbean carbonate crash, occurred at a periodicity of 400–500 k.y. and are emphasized in Figure 11 by the shaded bars. Carbonate content recovers to pre-crash levels by 10 Ma.

The overall pattern of the carbonate change observed in Hole 999A is surprisingly similar to the one described earlier in Hole 998A. However, there are some subtle differences between the two holes. As in Hole 998A, a gradual but more rapid decrease in carbonate content is observed before the onset of the carbonate crash. The slow decline of carbonate content ranges from 75 wt% at ~13.9 Ma to 55 wt% at the onset of the crash at ~12.1–12.0 Ma (Fig. 11B). However, this precursor to the crash is more conspicuous in Hole 999A because the carbonate decrease prior to 12 Ma is steeper and punctuated by a series of carbonate values lower than 40 wt%. This series of significant carbonate reductions are approximately spaced at a periodicity of 100–200 k.y., particularly in the interval from 13.6 to 12.5 Ma. Within the carbonate-crash interval, high-amplitude carbonate fluctuations are observed in Hole 999A (Fig. 11B). The ages at which the carbonate contents dip below 10 wt% within the highly variable carbonate-crash interval are 12.0, 11.6–11.4, 11.2–11.1, 11.0–10.8, and 10.1 Ma, similar to the five episodes observed in Hole 998A. Carbonate content recovers from the crash beginning at 10.0 Ma with the exception of one more interval of reduced carbonate weight percent at 9.4–9.2 Ma.

The carbonate-content values in Hole 1000A are as high as ~90 wt% at 13.8 Ma, but then drop to 70 wt% by 10.9 Ma, before increasing again to 90 wt% by 9.0 Ma (Fig. 11C). Superimposed on the general trend are highly variable carbonate contents with several minima at ~72 wt% prior to 13.8 Ma and decreasing below 65 wt% at 12.6, 12.4–12.3, 12.2, 12.0, 11.7, 11.5, 11.1, 10.9, 10.5, 10.2, and 10.0 Ma. Two additional minima occur at 9.8 and 9.4 Ma. With the exception of these latter two minimum values, the carbonate-content values following the carbonate crash do not experience the same degree of variation as seen in the carbonate content prior to the carbonate minimum.

Similarities between the pattern of carbonate-content variation among the three sites were compared statistically. Correlation coefficients and variables derived to test for the significance of the correlation coefficient are listed in Table 3. Based on the test for significance outlined by Swan and Sandilands (1995), the carbonate-content curves for Holes 998, 999, and 1000 are correlated between one another and the null hypothesis is rejected at 99% confidence.

Carbonate Mass Accumulation Rates

The carbonate records in Figures 9 and 11 display the variations of weight percent $CaCO_3$ relative to the bulk sample. In an effort to minimize the effect of carbonate dilution by noncarbonate components, CO_3 MARs were also calculated (Fig. 12). Prior to the carbonate crash, the CO_3 MARs averaged 0.75 g/cm^2 per k.y. and remained

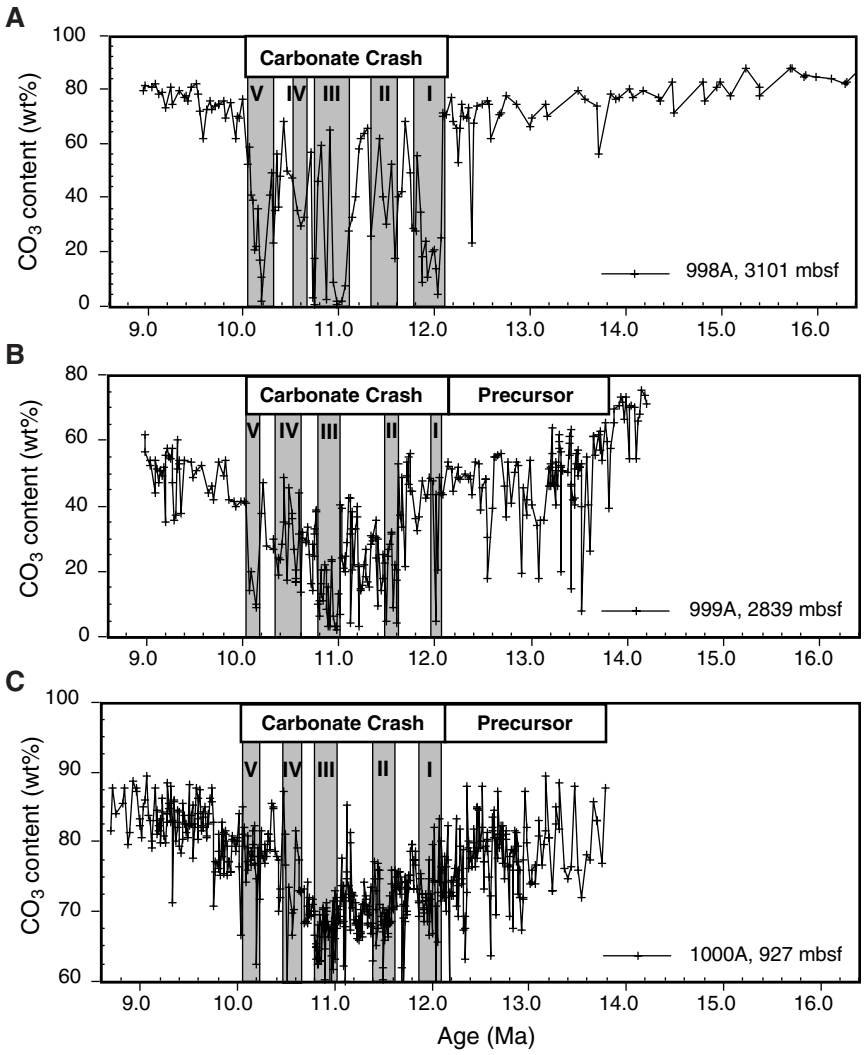

Figure 11. Shipboard and Rice University carbonate-content combined data sets. Note that the vertical axes have been scaled to emphasize the timing of the lowest carbonate-content values between the three sites. **A.** Hole 998A. **B.** Hole 999A. **C.** 1000A. Five carbonate-dissolution episodes (I–V) are identified and emphasized by the shaded column. The interval of the bundled five episodes, synchronous between the three Sites 998, 999, and 1000, is referred to as the Caribbean carbonate crash, which lasted for ~2 m.y. Note that times with low carbonate values are already observed prior to the onset of the carbonate crash in Holes 999A and 1000A, an interval referred to here as the carbonate precursor. This pattern contrasts with the one observed at Site 998, where no significant carbonate precursor is observed. Similarities in the pattern of the carbonate-content variations between the three sites were compared statistically (see Table 3).

constant in Hole 998A (Fig. 12A). Carbonate accumulation then dropped to almost 0 g/cm^2 per k.y. at 12.0 Ma (Fig. 12A). Accumulation rates remained low and highly variable throughout the 2 m.y. of the carbonate crash. Within this period, the CO_3 MAR oscillated between zero and 0.7 g/cm^2 per k.y. Five episodes during which only trace amounts or no carbonate accumulation are observed occurred at 12.1–11.8, 11.6–11.3, 11.1–10.8, 10.6–10.5, and 10.3–10.1 Ma. By 10 Ma, the carbonate accumulation rates recovered to precrash levels.

The pattern in carbonate accumulation rates in the Colombian Basin (Site 999) is very similar to that of the Yucatan Basin (Site 998) (Fig. 12A, B). The higher sedimentation rates at Site 999 (2.09 cm/k.y.), twice as high as the rates at Site 998 (0.92 cm/k.y.), translate into overall higher CO_3 MAR at Site 999. In Hole 999A, CO_3 MARs gradually decrease prior to the carbonate crash. The decline is observed from the beginning of the data set at 14.2 Ma but especially after 13.8 Ma with a CO_3 MAR of nearly 2.0 g/cm^2 per k.y. to 1.0 g/cm^2 per k.y. prior to the onset of the carbonate-crash interval at ~12.1 Ma (Fig. 12B). The carbonate-crash interval is characterized by high-amplitude variations in the CO_3 MAR and ends at 10.0 Ma. Similar to Site 998, significantly lower accumulation rates occur at near 12.0, 11.6–11.5, 11.0–10.8, and 10.2–10.1 Ma (Fig. 12B). However, the CO_3 MAR full recovery is only reached after ~9.4 Ma, a date that also postdates the nadir of the carbonate-crash interval in the eastern equatorial Pacific. Although most of the decreased CO_3 MARs occur during the 2-m.y. period of the carbonate crash, significant drops of CO_3 MAR are already observed in the time prior to the crash at 13.55, 13.05, and 12.55 Ma. These episodes of low CO_3 MAR appear to occur at a frequency of ~500 k.y. (Fig. 12B). Miocene carbonate cyclic variations at the frequency of 400–500 k.y. have been reported in deep-sea sediments in other parts of the Atlantic Ocean (e.g., Zachos et al., 1997). These earlier precursors of CO_3 MAR reductions observed in Hole 999A do not occur in Hole 998A (Fig. 12A), possibly because of the partial isolation of the Yucatan Basin from the southern Caribbean basins.

The CO_3 MAR in Hole 1000A (927 m of water depth) is much higher than at the two deeper Sites 998 and 999, with values ranging from ~3.0 to 5.5 g/cm^2 per k.y. (Fig. 12C). The lowest CO_3 MAR in Hole 1000A is, therefore, significantly higher than the highest CO_3 MAR in Holes 998A and 999A. These very high CO_3 MARs can be

Table 3. Correlation coefficient of carbonate content among Sites 998, 999, and 1000.

Sites	r	*t*	Critical *t*
998 and 999	0.604	4	2.3
998 to 1000	0.542	8	2.3
999 to 1000	0.505	10	2.3

Notes: r = correlation coefficient. *t* and critical *t* are variables used to determine correlation significance according to Swan and Sandiman (1995).

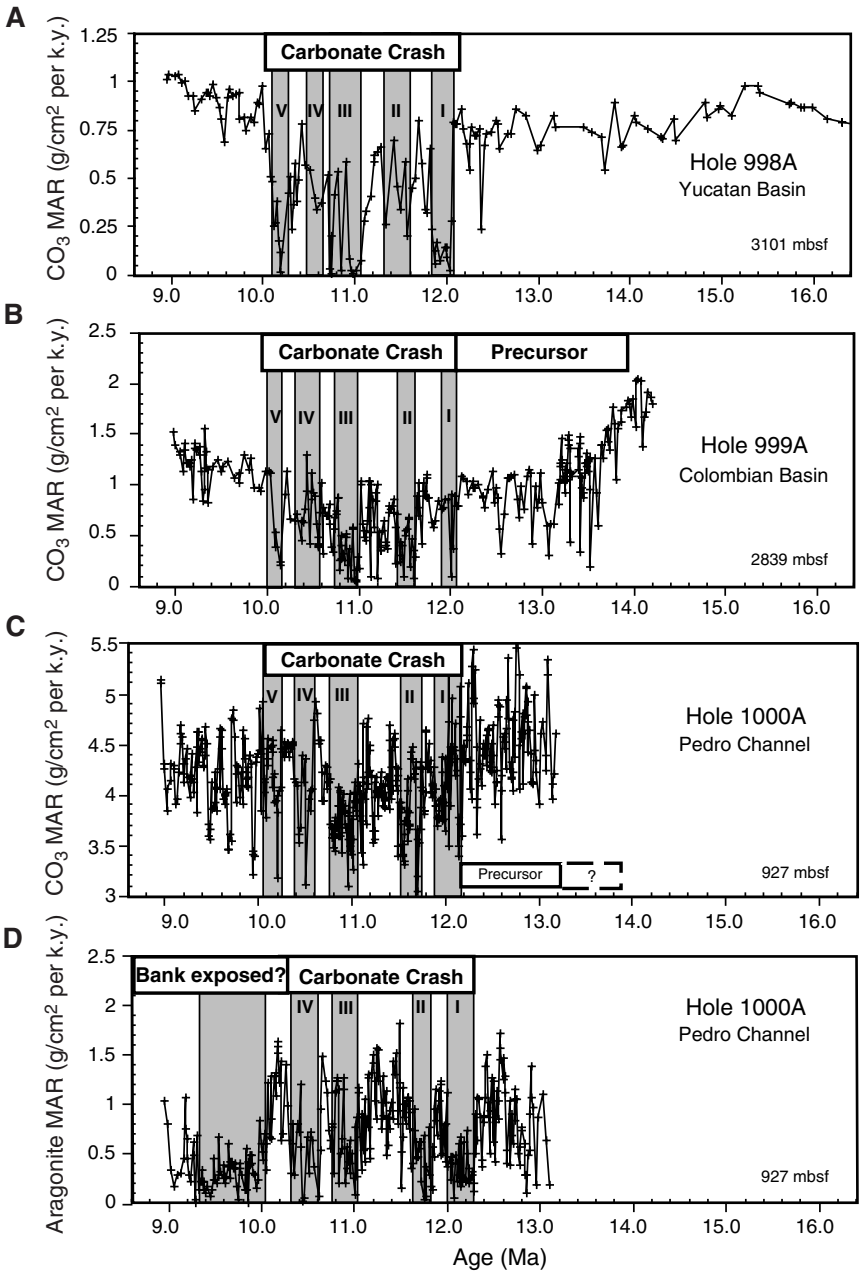

Figure 12. Carbonate mass accumulation rates (CO_3 MARs) for (**A**) Hole 998A, (**B**) Hole 999A, and (**C**) 1000A. As in Figure 11, five carbonate-dissolution episodes (I–V) are identified and emphasized by the shaded column. The interval of the bundled five episodes, approximately synchronous between the three Sites 998, 999, and 1000, is referred to as the Caribbean carbonate crash, which lasted for ~2 m.y. Note that times with low-carbonate MARs are already observed prior to the onset of the carbonate crash in Holes 999A and 1000A, an interval referred to here as the carbonate precursor. This pattern contrasts with the one observed at Site 998, where no carbonate precursor is observed. **D.** Aragonite MAR. The first four episodes characterized by low-aragonite MAR episodes in Hole 1000A are nearly contemporaneous with the carbonate-dissolution intervals observed in Holes 998A, 999A, and 1000A. The younger low-aragonite MAR episode (10–9.3 Ma) in Hole 1000A is unusually long and occurred when the CO_3 MAR had already recovered following the carbonate crash. This interval of low-aragonite MAR perhaps corresponds to an interval when the carbonate bank tops adjacent to Site 1000 were exposed because of low sea level and, therefore, were not producing a large volume of neritic carbonate.

explained by the shallow depth of Site 1000 and by its proximity to shallow carbonate platforms that shed large volumes of neritic aragonite and perhaps magnesian calcite–rich sediment to the adjacent basins. Similar to Sites 998 and 999, the carbonate-crash interval between 12 and 10 Ma in Hole 1000A is characterized by an overall lower CO_3 MAR and a series of high amplitude (1.5 g/cm^2 per k.y.) variations in CO_3 MAR. As at Site 998, and in particular at Site 999, episodes characterized by significantly lower CO_3 MARs occur at 12.1–11.9, 11.6–11.5, 11.1–10.8a, and 10.2–9.9 Ma (Fig. 12C).

Carbonate Mineralogy and Aragonite Mass Accumulation Rates

X-ray diffraction reveals the presence of aragonite in Hole 1000A. The aragonite component of the carbonate fraction in Hole 1000A was most likely produced on adjacent carbonate bank tops and exported offshore to the Site 1000 location. The production and, therefore, the export of bank-derived aragonite and magnesian calcite is tied to bank-top flooding and directly linked to sea-level fluctuations (e.g., Droxler et al., 1983; Schlager et al., 1994, and references therein). Because a magnesian calcite peak could not be detected from the low magnesian calcite peak, magnesian calcite is probably absent or only present in trace amounts. Because aragonite is metastable relative to low magnesian calcite, the water column becomes undersaturated with respect to aragonite at much shallower depths than does low magnesian calcite (Droxler et al., 1991). Aragonite MAR is a reliable proxy for carbonate preservation/dissolution (Schwartz, 1996). Figure 12D shows variations in aragonite MAR from 13.1 to 8.9 Ma in Hole 1000A. The points of lowest aragonite MAR occur at 13.1–12.9, 12.3–12.0, 11.8–11.6, 11.1–10.8, 10.6–10.3, and 10.0–9.3 Ma. The first four episodes of reduced aragonite accumulation during the interval of the carbonate crash correspond

relatively well to the first four episodes of carbonate reduction observed in Holes 998A, 999A, and 1000A (Fig. 12). However, the youngest 0.7-k.y.-long interval (between 10 and 9.3 Ma), characterized by reduced aragonite accumulation, occurs at a time when the carbonate had already fully recovered. This interval of low-aragonite MAR could be explained by an overall sea-level lowstand at the beginning of the late Miocene (Haq et al., 1987). As shown below in the isotope result section, this interval corresponds to some relatively heavy $\delta^{18}O$ values at Sites 998 and 999 (Fig. 13), likely corresponding to a marked sea-level lowstand.

Benthic Isotopes

Zero to 20 tests of *P. wuellerstorfi* were found in samples with an average of three per sample. Some of the samples in Holes 999A and 1000A were too indurated to allow separation of coarse from bulk samples; therefore, O and C isotopes are available only for some part of the upper middle/lower upper Miocene in those holes. Diagenetic effects on measured isotopes, if present, would likely alter the oxygen isotopes. However, because the $\delta^{18}O$ values derived from these samples are quite similar to contemporaneous values of compiled $\delta^{18}O$ records of J.C. Zachos (unpubl. data), the values of both $\delta^{18}O$ and $\delta^{13}C$ that are included in this study appear to have been spared from significant diagenetic alteration and are thought to be valid.

$\delta^{18}O$

In waters below the thermocline, the oxygen isotope ratio incorporated into benthic foraminifer tests is influenced to a lesser extent by temperature fluctuations. Oxygen isotope values in this study, therefore, are expected to reflect changes in ice volume and serve as a good proxy for eustatic sea-level changes.

In spite of the low time resolution of the isotopic data set in Hole 998A, an overall increase of the $\delta^{18}O$ values is clearly observed from 15.5 to 9 Ma (Fig. 13A). The $\delta^{18}O$ values in Hole 998A, as light as ~0.8‰ at 15.5 Ma, (Fig. 13A), become progressively heavier, reaching ~2.5‰ at 9 Ma. In Hole 999A, the $\delta^{18}O$ record is limited to the interval between 11.6 and 9 Ma (Fig. 13B). It is reassuring that the range of $\delta^{18}O$ values (from 1.2‰ to 2.3‰) in this interval in Hole 999A is similar to the range observed in Hole 998A (Fig. 13A, B). A gradual increase in $\delta^{18}O$ values is also observed in both holes from 10 to 9.0 Ma, with some of the heaviest $\delta^{18}O$ values between 9.4 and 9.0 Ma. The heaviest $\delta^{18}O$ values in Hole 999A are observed in a short interval between 11.4 and 11.2 Ma.

As expected because of the relative shallow depth of Site 1000, the benthic foraminifer $\delta^{18}O$ values in Hole 1000A, ranging from 0.65‰ to 1.78‰, are overall lighter than those in Holes 998A and 999A (Fig. 13C). Because coccolith plates and planktonic foraminifers dominate the calcareous portion of the bulk sediment and their tests are mineralized close to the ocean surface, the bulk sample $\delta^{18}O$ values in Hole 1000A are considerably lighter than the benthic values in the same hole by ~3.0‰. The four $\delta^{18}O$ records in Holes 998A, 999A, and 1000A display a plateau of $\delta^{18}O$ values between 12.4 and 10 Ma, varying within a 1.0‰ range and systematically shifted relative to the water depth of the sites and the nature of the analyzed material.

$\delta^{13}C$

The $\delta^{13}C$ at Sites 998 and 999 ranges from 1.5‰ to 0.1‰ (Fig. 14A, B). In Hole 998A, the data set spans a 6-m.y.-long interval be-

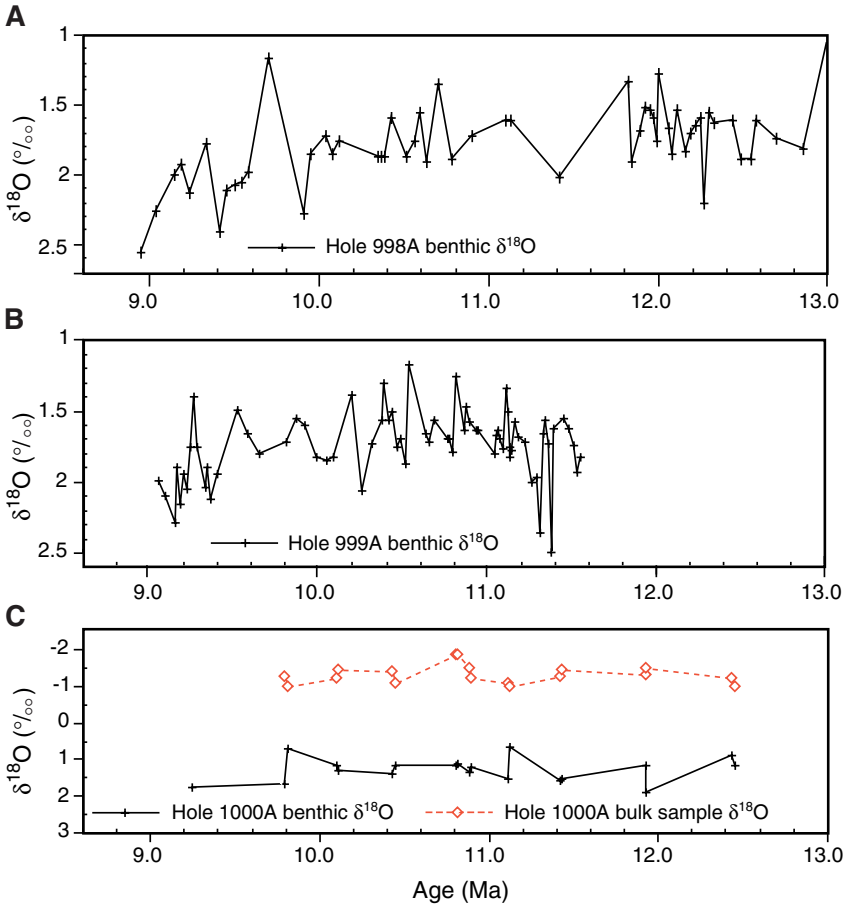

Figure 13. Variations of benthic $\delta^{18}O$ in Holes (**A**) 998A, (**B**) 999A, and (**C**) 1000A. Bulk sample $\delta^{18}O$ was also analyzed in Hole 1000A.

tween ~15 and 9 Ma and illustrates an overall trend where the heaviest values are observed in the intervals older than 13 Ma and younger than 9.5 Ma, loosely bracketing the carbonate-crash interval. Most of the lighter values in Hole 998A occur during the carbonate-crash interval and reach 0.6‰ ± 0.1‰ at 13.6, 12.3, 12.05, 11.8, 10.7, and 10.5 Ma, at times when the CO_3 MARs are minimum (Fig. 14A). However, these lightest $\delta^{13}C$ values might not be representative of the five episodes characterized by some of the lowest CO_3 MARs because benthic foraminifers are usually absent in the samples. It may be possible that the $\delta^{13}C$ for these episodes decreased to values as light as the lightest two values (~0.3‰) in Hole 998A, surprisingly observed in a short interval between 9.8 and 9.6 Ma during which the CO_3 MARs are among the highest observed rates (~1.5 g/cm^2 per k.y.).

Because samples older than 11.5 Ma in Hole 999A are highly indurated, the benthic $\delta^{13}C$ isotopic data set for Site 999 is limited to the interval between 11.5 and 9 Ma. Within the carbonate-crash interval in Hole 999A, the $\delta^{13}C$ values fluctuate between 0.1‰ and 1.4‰, while the $\delta^{13}C$ values in Hole 998A vary only between 0.3‰ and 1.1‰. The lightest $\delta^{13}C$ values (~0.1‰–0.3‰) in Hole 998A are found at 11.15, 10.9, 10.55, 9.85, and 9.35 Ma (Fig. 14B). Most of these lighter values in Hole 998A occur during some episodes within the carbonate-crash interval. However, as in Hole 998A, the interval characterized by some light values between 10.05 and 9.6 Ma corresponds to a time when the CO_3 MAR had already recovered subsequently to the carbonate-crash interval.

Only a limited number of samples from Hole 1000A were analyzed for their benthic $\delta^{13}C$ because of their overall high degree of induration. With the exception of the lightest $\delta^{13}C$ value of –0.71‰, the range of the $\delta^{13}C$ values in Hole 1000A, 1.31‰–0.0‰, is about equivalent to the range observed in Hole 999A (Fig. 14C). The samples with the lightest values occur at 11.9, 11.4, and 10.8 Ma, within some of the episodes of the carbonate-crash interval (Fig. 14C). The most negative and lightest $\delta^{13}C$ value at 11.9 Ma can be related to the water depth (927 m) of Site 1000, probably within the oxygen minimum zone, a level usually characterized by some of the lightest $\delta^{13}C$ in the water column.

DISCUSSION

In the late middle Miocene, dramatic change in the nature of water masses filling the Caribbean basins was recorded by five episodes of greatly reduced carbonate accumulation (Figs. 11, 12). Because these five episodes, identified by a decline in the carbonate content and MAR, are characterized by a decreased preservation of planktonic foraminifers and usually a smaller coarse-fraction proportion, they are interpreted to correspond to carbonate-dissolution episodes triggered by a major oceanic perturbation in the Caribbean that lasted ~2 m.y. (from ~12 to 10 Ma). The interval including the five carbonate-dissolution episodes is referred to as the Caribbean carbonate crash. While the term "carbonate crash" was borrowed from ODP Leg 138

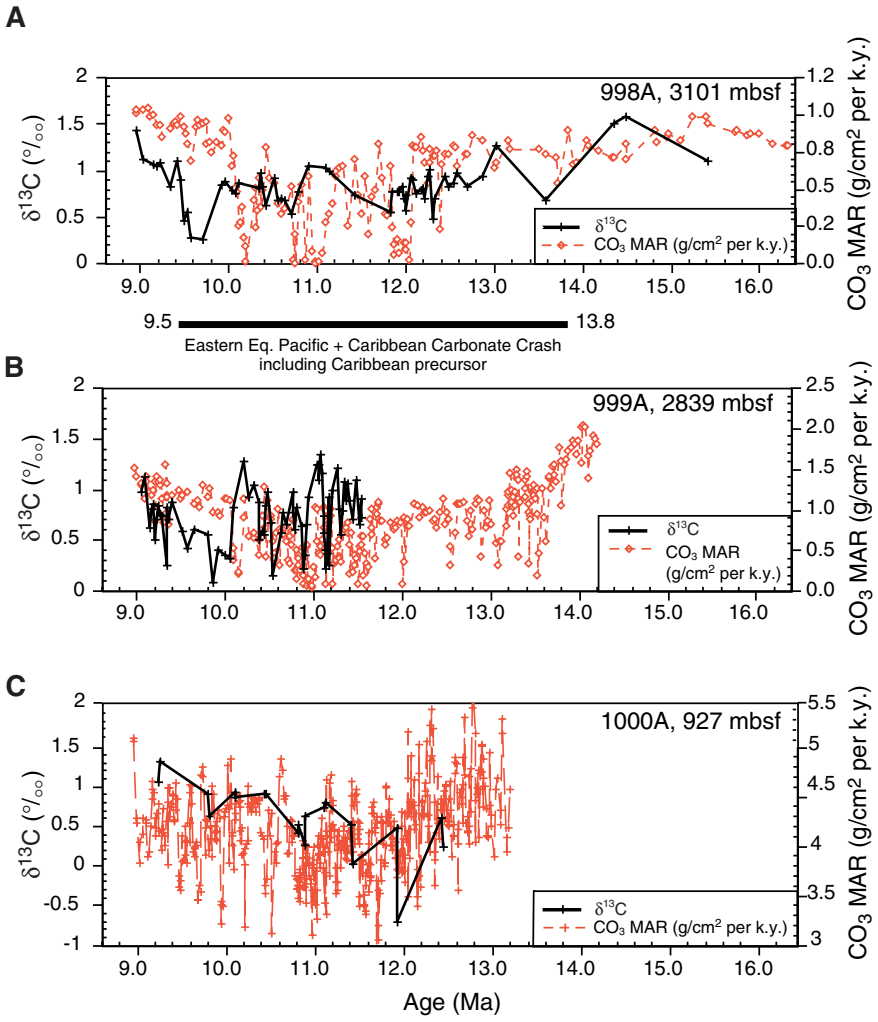

Figure 14. Variations of benthic $\delta^{13}C$ compared to carbonate mass accumulation rates (CO_3 MAR) in Holes (**A**) 998A, (**B**) 999A, and (**C**) 1000A.

published results (Lyle et al., 1995), we also acknowledge here that the respective timing of the carbonate-dissolution interval observed in the Pacific and Caribbean at the middle to late Miocene transition did not fully overlap. The third of the five carbonate Caribbean dissolution episodes (Figs. 11, 12) appears to be contemporaneous with the onset of the main carbonate dissolution in the eastern equatorial Pacific Ocean (Figs. 1, 15). In this discussion, we will attempt to show that the interplay between the seaway opening along the northern Nicaraguan Rise and the gradual closure of the Central American Seaway resulted in the initiation of the Caribbean and Loop Currents, the strengthening of the Gulf Stream, and, as a consequence, the re-establishment and intensification of the NADW production. We will try to demonstrate that this scenario can explain the simultaneous occurrence of the carbonate crash on either side of the Isthmus of Panama.

The results of this study show that the Caribbean carbonate crash reaches its zenith during an interval between 12 and 10 Ma when the connection between the southern and northern Caribbean basins (Colombian and Yucatan Basins) was finally established through the opening of several seaways along the northern Nicaraguan Rise and the contemporaneous gradual closing of the Central American Seaway to intermediate depths (Figs. 2, 4, 5). The temporary complete closure of the Central American Seaway between ~10.0 and 9.5 Ma (Fig. 2), possibly tied to a major lowering of sea level during this interval (Haq et al., 1987) (Fig. 13A, B), appears to correspond to the zenith of the carbonate crash in the eastern equatorial Pacific (Figs. 1, 15D) and, in the deep Caribbean basins, to some relatively heavy $\delta^{18}O$ values (Fig. 13), the lightest benthic $\delta^{13}C$ (Fig. 14), and an interval characterized by the sustained lowest aragonite MAR in Hole 1000A (Fig. 12D). Surprisingly, during the same time interval, the carbonate system had already fully recovered in the Caribbean basins. In this discussion, the previous models to explain the carbonate crash in the eastern equatorial Pacific Ocean (Lyle et al., 1995) are summarized. Then, a model modified from the one published by Lyle et al. (1995) will be proposed to explain the occurrence of the carbonate crash on both sides of the Isthmus of Panama. This model is based on an analogy with a carbonate model proposed by Haddad and Droxler (1996) to explain the late Quaternary glacial/interglacial carbonate preservation pattern in the Caribbean basins.

Previous Models for the Middle to Late Miocene Carbonate Crash

Lyle et al. (1995) attributed the carbonate crash observed in ODP Leg 138 Neogene pelagic sequences of the eastern equatorial Pacific (Figs. 1, 15D) to the emergence of the Isthmus of Panama. Although the isthmus was still below sea level for most of the time of the crash, they calculated that a restriction of 2 Sv (1 Sv = 1×10^6 m^3/s) of carbonate-rich deep and intermediate water masses from the Atlantic to the Pacific would account for the loss of carbonate accumulation on the equatorial part of the East Pacific Rise and west of the isthmus. However, because this scenario does not restrict the flux of carbonate-rich deep and intermediate water masses in the Caribbean Sea, the occurrence of the carbonate crash in the Caribbean basins, discovered subsequent to Lyle et al. (1995) by Sigurdsson, Leckie, Acton, et al. (1997), cannot be explained by this model.

Lyle et al. (1995) also proposed a second model to explain the carbonate crash in the eastern Pacific. This latter model involves changing the global deep-ocean circulation triggered by the onset of deep-water production in the high latitudes of the North Atlantic Ocean, a scenario analogous to the modern oceanographic setting of deep-water circulation. Accordingly, the initiation of NADW would cause a reorganization of deep-water circulation and would affect the carbonate preservation in the eastern equatorial Pacific. The initiation and the strengthening of NADW flow would compete with the Antarctic Bottom Water (AABW) in the South Atlantic, resulting in the displacement of some of the more corrosive AABW toward the Pacific, triggering more dissolution in the eastern equatorial Pacific. Lyle et al. (1995) were in favor of the closing of the Central American Seaway as the mechanism responsible for the carbonate crash at the middle to late Miocene transition. The role of the NADW establishment and intensification in influencing the carbonate preservation and accumulation in the eastern equatorial Pacific Ocean was not clear prior to the discovery that the carbonate crash occurred at about the same time on both the Caribbean and Pacific sides of the Isthmus of Panama (Sigurdsson, Leckie, Acton, et al., 1997). The partial and perhaps temporary complete closure of the Central American Seaway at the middle to late middle Miocene transition, in addition to decreasing the flow of carbonate-rich intermediate waters from the Atlantic to the Pacific, may also have directly influenced the NADW production. Constraining the timing and observing the pattern of carbonate accumulation on both sides of the Isthmus of Panama should help us to develop a scenario to explain the occurrence of the carbonate crash at the middle to late Miocene transition.

The model proposed here to explain the occurrence of the Caribbean carbonate crash draws on the circulation changes induced by the re-establishment and intensification of the NADW (or its precursor, NCW). We propose that the carbonate crash in the Caribbean Sea and the eastern equatorial Pacific Ocean resulted from a global reorganization of the thermohaline oceanic circulation at the middle to late Miocene transition. The re-establishment (Fig. 15E) (Wright and Miller, 1996) and/or the initiation (Wei and Peleo-Alampay, 1997) of the NADW production at this time caused an influx of corrosive AAIW entering the Caribbean basins and ultimately resulted in dramatic seafloor dissolution of calcareous sediments. This hypothesis is built upon an analogy with the late Quaternary glacial to interglacial perturbations of the global thermohaline circulation and their related results in terms of carbonate sediment accumulation in the Caribbean basins (Haddad and Droxler, 1996). Moreover, we further propose that the middle Miocene drowning of carbonate banks in the northern part of the Pedro Channel and Walton Basin along the northern Nicaraguan Rise (Figs. 4, 5) was contemporaneous to the partial closing of the Central American Seaway, and thus would have played a significant role in triggering the global reorganization of the oceanic circulation (Droxler et al., 1998).

Proposed Model for the Caribbean Carbonate Crash

Our model for the Caribbean carbonate crash proposes that the re-establishment and intensification of the NADW in the late middle Miocene (Wright and Miller, 1996) were triggered by the opening of seaways along the northern Nicaraguan Rise, creating a connection between the Colombian and Yucatan Basins (Figs. 2B, 5) (Droxler et al., 1998). These events were contemporaneous with the closure at intermediate- and deep-water levels of low-latitude seaways connecting the Atlantic and the Pacific oceans (Fig. 2) (Duque-Caro, 1990). Prior to significant NADW production in the early middle Miocene (Fig. 15E) (Wright and Miller, 1996), AABW was the main source of deep water and, because it formed in the Southern Ocean. AABW could directly fill all three major ocean basins as far north as the north latitudes of the Atlantic and Pacific oceans. Once the production of NADW was established and subsequently intensified, large volumes of deep waters were formed in the North Atlantic. Without a low-latitude connection at bathyal and abyssal depths between the Atlantic and the Pacific, the NADW had to travel the length of the Atlantic and around the perimeter of Antarctica before entering the Pacific. This quasi-unidirectional flow, as the modern thermohaline conveyor, resulted in a case of basin-to-basin fractionation between the carbonate-rich Atlantic and carbonate-poor Pacific oceans (Berger, 1970a; Gordon, 1986; Broecker et al., 1990).

Despite NADW's chemistry, which promotes calcium carbonate preservation, carbonate sediment is dissolving in the Caribbean today

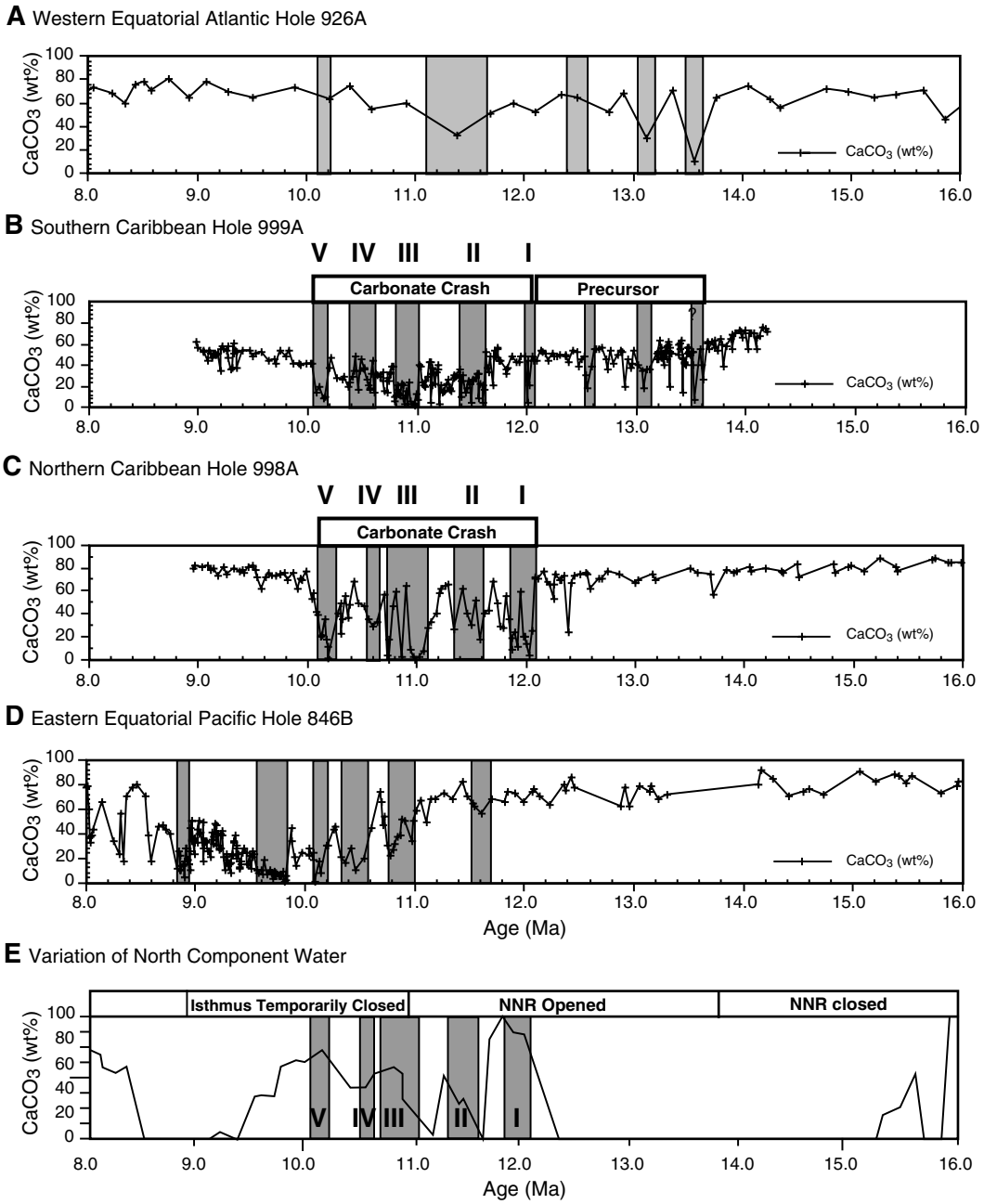

Figure 15. Variations of carbonate-content values between 16 and 8 Ma in three different areas of the globe. **A.** Hole 926A from the Ceara Rise in the equatorial Atlantic, Leg 154 (Curry, Shackleton, Richter, et al., 1995). **B.** Hole 999A in the Colombian Basin (see Fig. 9). **C.** Hole 998A in the Yucatan Basin (see Fig. 9). **D.** Hole 846A from the eastern equatorial Pacific, Leg 138 (Pisias, Mayer, Janecek, Palmer-Julson, van Andel, et al., 1995). **E.** Variations of North Component Water production in the North Atlantic from Wright and Miller (1996). NNR = northern Nicaraguan Rise. Stippled columns in B, C, D, and E correspond to intervals of reduced carbonate values that include the five episodes of carbonate dissolution (I–V) observed during the Caribbean carbonate crash (see Figs. 11, 12). The timing of these episodes corresponds surprisingly well with the peaks of North Component Water production in the North Atlantic. Columns with lighter shading in A represent dissolution inferred through reduced coarse fraction in Hole 926A (Shackleton and Crowhurst, 1997). In B, three of these intervals are synchronous with three episodes of carbonate dissolution in Hole 999A that occurred during the carbonate crash precursor. The initial carbonate decrease in Hole 846B in the eastern equatorial Pacific (shown in D) at ~11 Ma corresponds to the Caribbean dissolution Episode III (shown in B and C). Episodes IV and V in B and C correspond to intervals of low carbonate values in Hole 846B. Note that the interval characterized by the lowest carbonate values between 9.8 and 9.5 Ma in Hole 846B, the nadir of the carbonate crash in the eastern equatorial Pacific, occurred at a time when the carbonate system had already recovered in the Caribbean basins.

when the production of NADW is at its maximum (Figs. 6A, 16A). We propose that this is as it was during the Caribbean late middle Miocene carbonate crash, a time when NADW was newly being re-established (Wright and Miller, 1996). The changes of oceanic circulation at the transition from the middle to late Miocene can be illustrated by using the late Quaternary glacial–interglacial circulation and carbonate preservation patterns in the Caribbean as an analogue to "pre-carbonate crash"–"height of carbonate crash" periods. During the late Pleistocene glacial stages (Gordon, 1986; Broecker et al., 1990; Raymo et al., 1990), as it may have been during the early middle Miocene (Wright et al., 1992; Wright and Miller, 1996), the production of NADW was significantly reduced or had completely ceased and calcium carbonate was preserved in both the eastern equatorial Pacific Ocean and the Caribbean Sea (Fig. 16A) (Lyle et al., 1995; Le et al., 1995; Sigurdsson, Leckie, Acton, et al., 1997; Haddad and Droxler, 1996). The water mass entering the Caribbean over bathyal sill depths during the last glacial maximum and perhaps during the pre-crash early middle Miocene interval was a well-oxygenated and relatively heavy $\delta^{13}C$ glacial North Atlantic Intermediate Water (Slowey and Curry, 1995; Haddad and Droxler, 1996) (Figs. 6B, 16). With the NADW being significantly reduced, the Southern Ocean then dominates deep-water production (Fig. 6B). As a consequence, the eastern equatorial Pacific deep waters were relatively young and well oxygenated and consequently noncorrosive to carbonate (i.e., Le et al., 1995, and references herein)

In the Holocene, as may also have been the case at the nadir of the middle to late Miocene carbonate crash, especially during the five episodes of massive carbonate dissolution in the Caribbean basins (Figs. 11, 12), NADW was well developed, and carbonate dissolution is observed on both sides of the Isthmus of Panama in the eastern equatorial Pacific and in the Caribbean Sea during an interval from ~11 to 10 Ma (Fig. 15). Using a composite dissolution index based on metastable carbonate, Haddad and Droxler (1996) linked late Quaternary increases of NADW production with greater dissolution of calcium carbonate in the Caribbean Sea (Fig. 16A). The Caribbean carbonate crash between 12 and 10 Ma is interpreted to be related to a period of greater NADW production (Wright and Miller, 1996). When NADW is being produced, large volumes of water, equivalent to the amount sinking in the Norwegian and Labrador Seas and exiting the North Atlantic Ocean toward the Southern Ocean, are pulled northward through the Caribbean in the upper 1500 m of the water column to replenish the sinking water (Fig. 6A) (Schmitz and McCartney, 1993). This brings southern-sourced intermediate waters farther north during interglacial times than during glacial stages (Fig. 6). The carbonate-corrosive AAIW entrains the upper NADW when entering over the Caribbean sill depth. These waters fill the basins, causing increased dissolution in the Caribbean (Fig. 16) (Haddad and Droxler, 1996). In times of increased NADW production, such as during the Holocene–last interglacial Stage 5 and possibly at the middle to late Miocene transition, the eastern equatorial Pacific is farther from the northern source of deep-water production, causing its carbonate chemistry to be dominated by older, corrosive waters enriched in ΣCO_2. NADW production can be associated, therefore, with dissolution in the eastern equatorial Pacific Ocean (corrosive bottom/deep waters) as well as in the Caribbean basins (corrosive intermediate waters).

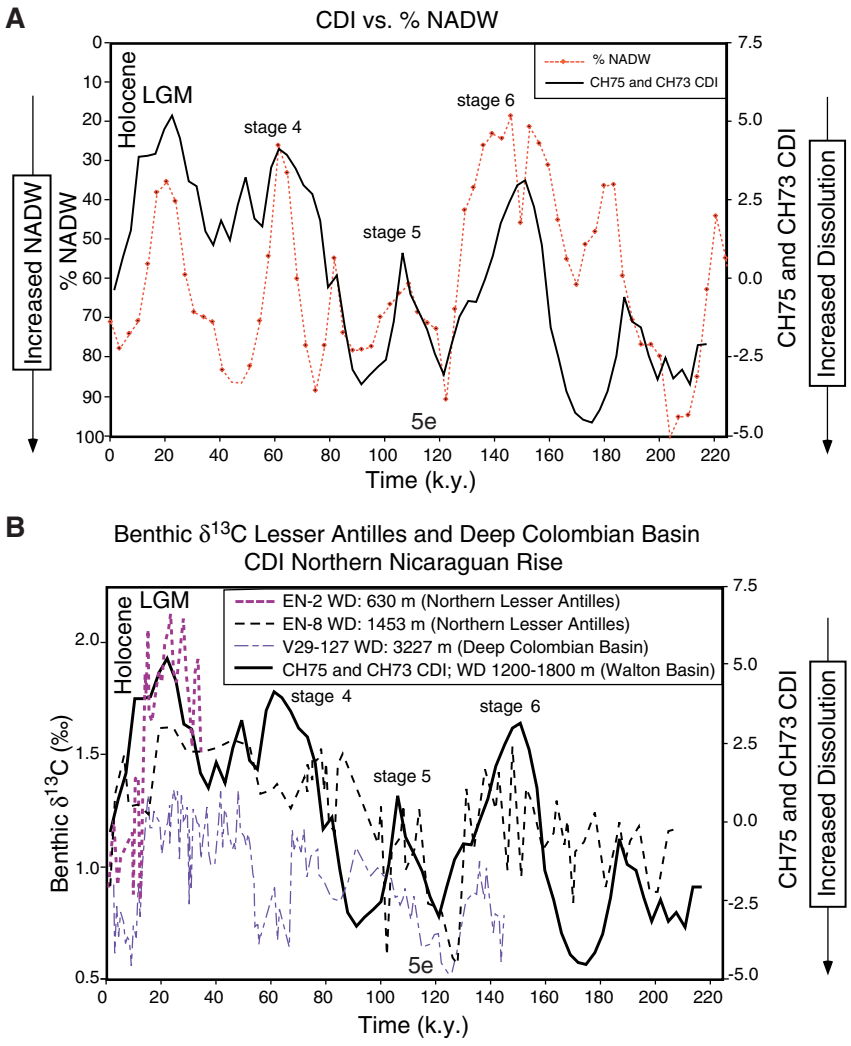

Figure 16. **A.** Correlation between fluctuation of North Atlantic Deep Water (NADW) production (from Raymo et al., 1990) and a carbonate composite dissolution index (CDI) from Walton Basin on the northern Nicaraguan Rise during the late Quaternary (Haddad, 1994; Haddad and Droxler, 1996). Note that maximum NADW production during the Holocene and last interglacial Stage 5e correlates with dissolution peaks in the Caribbean when the more corrosive Antarctic Intermediate Water flowed through the Caribbean. This late Quaternary interglacial scenario could illustrate the oceanographic setting in the Caribbean during the carbonate crash at the middle to late Miocene transition. On the other hand, the last glacial maximum (LGM) and previous glacial intervals are associated with dramatic reduction of NADW production and maximum carbonate preservation. This late Quaternary glacial scenario is a good illustration of the oceanographic setting prior to the Caribbean carbonate crash in the middle Miocene. **B.** Correlation between several benthic $\delta^{13}C$ records (Shearer et al., 1995; Oppo and Fairbanks, 1990) from subthermocline to abyssal depths in the Caribbean Basins and the carbonate CDI (see A; Haddad and Droxler, 1996). Lighter $\delta^{13}C$ values correspond to interglacial carbonate-dissolution intervals (Holocene and Stage 5e) when NADW was at its maximum and AAIW was flowing through the Caribbean basins. The LGM was a time of heavy $\delta^{13}C$, maximum carbonate preservation, and minimum NADW production. EN = Endeavour; CH = Cape Hatteras; WD = water depth.

Caribbean Gateways, Establishment of the Caribbean Current, and NADW Production

Maier-Reimer et al. (1990) use general circulation models (GCM) to show how changes in thermohaline circulation and NADW production can be tied to partial or full closure of the Isthmus of Panama. In their modern model with an emergent Isthmus of Panama, NADW is produced. In a second scenario, with a modeled open Central American Seaway, NADW production is inhibited. The GCM of Maier-Reimer et al. (1990) appears to demonstrate that a deeply submerged isthmus would be linked with a lack of NADW production. Mikolajewicz and Crowley (1997) supplemented those results with more GCM experiments that support NADW production to some degree already with a partially emergent isthmus, as is thought to be the case in the middle to late Miocene transition. So far, no models have been developed to demonstrate the possible effect of channel opening across the northern Nicaraguan Rise.

The modern thermohaline circulation pattern, characterized by deep-water formation in high latitudes of the Atlantic Ocean or North Component Water (NCW), was initiated as early as the late early Miocene (Fig. 15E) (Wright and Miller, 1996), but certainly by the late middle Miocene (Woodruff and Savin, 1989; Wei, 1995; Wei and Peleo-Alampay, 1997), with an interval in the early middle Miocene when the NCW was temporarily inhibited (Wright and Miller, 1996). The onset of the Caribbean carbonate crash, characterized by dramatic decreases in carbonate accumulation at Sites 998, 999, and 1000, appears to be synchronous with the main intensification (re-establishment) of the modern thermohaline circulation and may be directly linked to the reorganization of the oceanic water masses flowing through the Caribbean basins (Figs. 15, 17). An intensification of NADW at this time may be the result of the opening and partial closure of gateways in the Caribbean Sea during the middle Miocene.

Northern Nicaraguan Rise

One feature in the Caribbean thought to be prominent during the Oligocene to early Miocene is a series of carbonate banks and barrier reefs that spanned the distance from Nicaragua and Honduras to Jamaica (Figs. 4, 5) (Droxler et al, 1989, 1992, 1998; Lewis and Draper, 1990; Cunningham, 1998). This is the location of the modern northern Nicaraguan Rise (Fig. 3). The presence of these neritic banks during the early Miocene would have served as a barrier to northward water transport and would have also enhanced westward tropical flow between the Caribbean and the eastern Pacific (Fig. 5). Coccolith assemblages at Sites 998 and 999, north (Yucatan Basin) and south (Colombian Basin) of the northern Nicaraguan Rise, respectively, show minimal connection in the surface circulation between those two basins during nannozones CN3 and CN4 (16.2–13.57 Ma) (Fig. 2B) (Kameo and Bralower, Chap. 1, this volume; Kameo and Sato, in press). This observation supports the idea of a barrier impeding any significant surface flow over the northern Nicaraguan Rise in the early middle Miocene. Partial foundering of this barrier because of faulting, linked to rifting intensification in the Cayman Trough, may have started in the mid-Oligocene but mostly occurred in the early middle Miocene. Cunningham (1998) places the initiation of tectonic activity and mini-basin formation in the Pedro Channel area at 16–11 Ma (ages of Raffi and Flores, 1995). This activity may also be related to the change from a relatively long period of quiescence on the northern Nicaraguan Rise to the uplift of Jamaica in the late middle Miocene (Leroy et al., 1996). The demise of carbonate neritic banks in the northern part of Pedro Channel and the central part of Walton Basin has led to the observed modern configuration of shallow, carbonate banks segmented by north-south oriented channels (Fig. 4) (Cunningham, 1998; Droxler et al., 1998). The merging of coccolith assemblages between Sites 998 and 999 (Fig. 2B) (Kameo and Bralower, Chap. 1, this volume; Kameo and Sato, in press), was first initiated during nannozone CN5 (13.57–10.71 Ma) and was fully completed during nannozones CN6 and CN7 (10.71–9.36 Ma) and supports the estimated timing of a seaway opening along the northern Nicaraguan Rise.

Central American Seaway

Because of the episodic uplift history of the Panamanian isthmus (see Farrell et al., 1995), it is difficult to constrain the timing of the Central American Seaway closure. Duque-Caro (1990) dates the uplift to 1000 m (upper bathyal depths) at 12.9–11.8 Ma, based on benthic foraminiferal assemblages from onshore Colombian basins and the time scale of Keller and Barron (1983), which is equivalent to the 12–10.2 Ma of Raffi and Flores (1995) (Figs. 2A, 7). Kameo and Sato (in press) show that eastern Pacific coccolith assemblages remained identical to those of Site 999 in the Colombian Basin from 16.21–13.57 Ma, started to diverge at 13.57 Ma, and became very different between 10.71 and 9.36 Ma (Fig. 2B). Based upon the results of Duque-Caro (1990) and Kameo and Sato (in press), the flow of the upper water column was restricted through the Central American Seaway during the late middle Miocene while the surface mixed-layer flow through the seaway might have been temporarily closed for the first time sometime in the interval between 10.71 and 9.36 Ma at the middle to late Miocene transition. This temporary first closure of the Isthmus of Panama is recorded by the first intermingling of terrestrial faunas between the South and North American continents (Fig. 17) (Webb, 1985).

Establishment of the Caribbean Current

With the barrier across the northern part of the Pedro Channel subsided and the Isthmus of Panama partially uplifted, the Caribbean Current became established. Saline water from the southern Caribbean basins was for the first time transported northward into the Gulf of Mexico. The Loop Current, which connects the Caribbean water with the Gulf of Mexico, the Gulf Stream, and ultimately the northern North Atlantic (Fig. 6A), also became established at this time (15–12 Ma, Mullins et al., 1987; ages of Berggren et al., 1985, corresponding to ~14–11.5 Ma in the Raffi and Flores, 1995, time scale). The timing of the onset of the Loop Current in the Gulf of Mexico appears to correspond to the base of a large sediment drift in Santaren Channel, dated at ~12.4 Ma by Eberli et al. (1998) and thought to be linked to a major Gulf Stream intensification. Moreover, farther downstream along the western boundary current of the North Atlantic, Popenoe (1985) noted a pronounced unconformity in the late middle Miocene sediments of the Blake Plateau. The initiation of the sedimentary drift in the Santaren Channel and the unconformity on the Blake Plateau would correspond to the strengthening of the Gulf Stream in response to contemporaneous establishment of the Caribbean/Loop Current system. Timing of the re-establishment and intensification of NADW in the late middle Miocene appears to be contemporaneous to those changes along the North Atlantic western boundary current (Wright and Miller, 1996; Woodruff and Savin, 1989; Wei, 1995; Wei and Peleo-Alampay, 1997). The formation of the Caribbean/Loop Current system introduced for the first time a large volume of warm, saline waters from the Caribbean and the Gulf of Mexico to the high latitudes of the North Atlantic via the Florida Current and Gulf Stream. As established from the modern thermohaline circulation, these conditions are necessary for the formation of a deep-water mass in the high latitudes of the North Atlantic Ocean (Gordon, 1986; Schmitz and McCartney, 1993). If this scenario is correct, the Caribbean carbonate crash and the initiation of the Caribbean Current should be contemporaneous with the intensification of NADW.

In addition, prior to 12.1 Ma, the time of the onset of the Caribbean carbonate crash, a reduction of carbonate percent and accumulation rates is observed in the two southerly sites, Site 999 (Colombian Basin) and Site 1000 (Pedro Channel, northern Nicaraguan Rise) (Figs. 11, 12). We consider this early carbonate reduction as a precursor to the carbonate crash. The conspicuous absence of a carbonate-

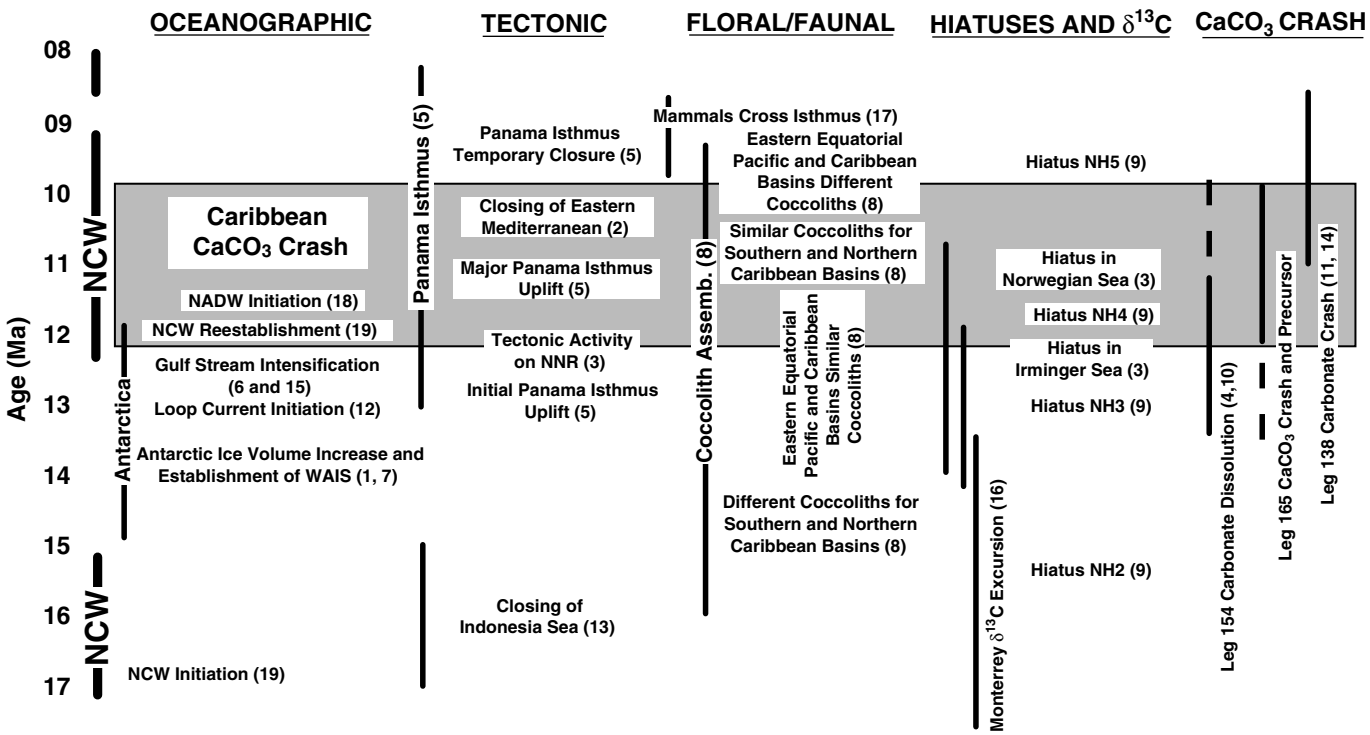

Figure 17. Summary chart of paleoceanographic, tectonic, floral, faunal, and sedimentary changes from the late early Miocene to early late Miocene. NCW = North Component Water; NADW = North Atlantic Deep Water; NNR = northern Nicaraguan Rise. (1) Abreu and Anderson, 1998; (2) Barron and Baldauf, 1989; (3) Cunningham, 1998; (4) Curry, Shackleton, Richter, et al., 1995; (5) Duque-Caro, 1990; (6) Eberli et al., 1998; (7) Flower and Kennett, 1994; (8) Kameo and Sato, in press; (9) Keller and Barron, 1983; (10) King et al., 1997; (11) Lyle et al., 1995; (12) Mullins et al., 1987; (13) Nishimura et al., 1997; (14) Pisias, Mayer, Mix, et al., 1995; (15) Popenoe (1985); (16) Vincent and Berger, 1985; (17) Webb, 1985; (18) Wei and Peleo-Alampay, 1997; and (19) Wright and Miller, 1996.

crash precursor in the northern Caribbean Site 998 (Yucatan Basin) may illustrate the isolation of the Yucatan Basin relative to the Colombian Basin and Pedro Channel prior to the carbonate crash itself. As noted earlier in our discussion, the presence of different coccolith assemblages on either side of the northern Nicaraguan Rise during the early middle Miocene (Fig. 2B) is another line of evidence to argue that the Yucatan Basin was isolated from the Colombian Basin and Pedro Channel prior to the onset of the Caribbean carbonate crash and that the Caribbean Current was not established at that time. The connection between the Colombian Basin, Pedro Channel, and the Yucatan Basin was probably only established by the first major carbonate-dissolution episode at ~12.1–12.0 Ma with the final subsidence of the reefal barrier in the northern part of Pedro Channel (Figs. 4, 5).

From 12.1 to 10.1 Ma, five episodes of carbonate dissolution are observed in all three Caribbean sites. During most of the five episodes, CO_3 MARs reach zero or slightly above zero in Holes 998A and 999A. These carbonate-dissolution episodes are likely caused by the influx of a southern-sourced, CO_2-rich, $\delta^{13}C$-depleted intermediate water mass, equivalent to the current AAIW, into the Caribbean over bathyal sill depth.

Benthic $\delta^{13}C$ Water Mass Signature

The $\delta^{13}C$ interbasinal gradient that exists today reflects the sources and pathways of intermediate- and deep-water masses. As intermediate- and deep-water masses age, the lighter ^{12}C isotopes (preferentially stored in organic tissues) are released in the waters through oxidation of the organic matter accumulating on the seafloor. This mechanism progressively lightens the $\delta^{13}C$ composition of intermediate- and deep-water masses until they are upwelled. Figure 18A shows the depth variations of the $\delta^{13}C$ values for the different oceans and in particular for the western Atlantic Ocean (Fig. 18B) (Kroopnick, 1980; 1985). A comparison between Figures 18B and 6A shows that each individual intermediate- and deep-water mass displays characteristic $\delta^{13}C$ values. The oxygen-enriched and nutrient-poor NADW is characterized by relatively heavy $\delta^{13}C$ (>1.0‰) when compared to the relatively light $\delta^{13}C$ (<0.8‰) oxygen-poor and nutrient-enriched AAIW (Fig. 18).

Predating and postdating the carbonate crash and during the intervening intervals of relatively high carbonate accumulation between the five carbonate-dissolution episodes, heavier $\delta^{13}C$ values (usually >1.0‰) are generally observed (Fig. 14). These heavier $\delta^{13}C$ values perhaps reflect the influence of oxygen- and carbonate-enriched and nutrient-poor intermediate-water masses formed in North Atlantic Ocean. This suggestion is based upon the analogy we are making between the carbonate-preservation pattern observed during the carbonate crash at the middle to late Miocene transition and the late Quaternary glacial–interglacial cycles. Carbonate sediments in the Caribbean basins are preferentially preserved during late Quaternary glacial stages when benthic $\delta^{13}C$ values are generally heavy and production of NADW reaches minimum values (Fig. 16B) (Haddad and Droxler, 1996).

The temporal resolution of the stable isotope data in Holes 998A, 999A, and 1000A varied due to the absence of the benthic foraminifer *Planulina wuellerstorfi* in many analyzed samples, especially the ones with very low carbonate-content values. In spite of a limited benthic carbon isotope data set in our Caribbean crash study, light $\delta^{13}C$ values, indicative of a nutrient-enriched intermediate-water mass in the Caribbean basins, appear to occur during the five episodes of massive carbonate dissolution during the carbonate-crash interval (Figs. 12, 14). In Hole 998A, benthic $\delta^{13}C$ light values of ~0.6‰ occur at ~12 Ma, the time of carbonate reduction Episode I and between 10.7 and 10.4 Ma (Episode IV) (Fig. 14A). Light benthic $\delta^{13}C$ values in Hole 999A occur at ~11 Ma (Episode III), ~10.6 Ma (Episode IV), and ~10 Ma (Episode IV). When compared to reduced

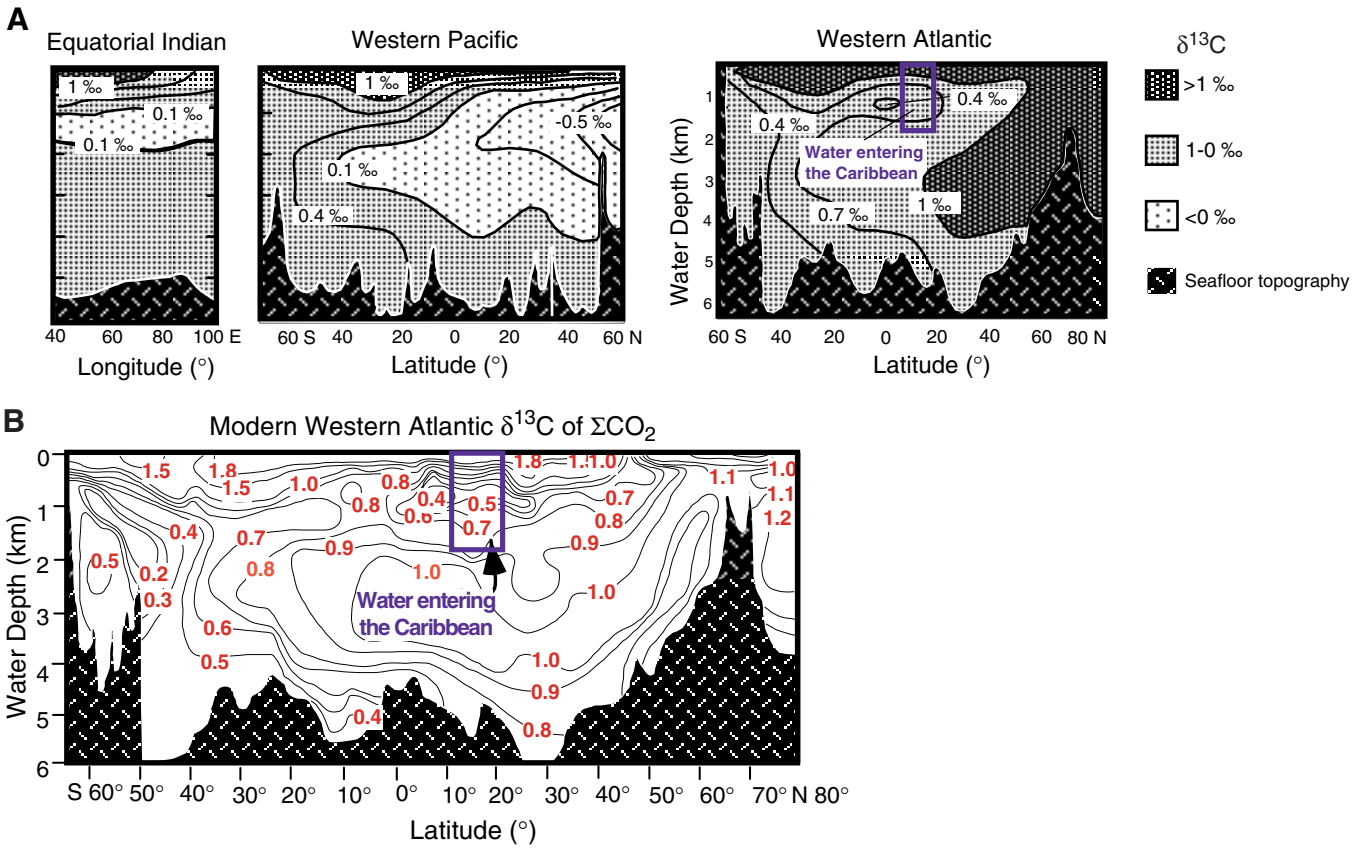

Figure 18. **A.** $\delta^{13}C$ of the modern equatorial Indian, western Pacific, and western Atlantic oceans (after Kroopnick, 1985; modified by Woodruff and Savin, 1989). **B.** Detailed $\delta^{13}C$ of the modern western Atlantic showing that the Antarctic Intermediate Water entering the Caribbean basins has low $\delta^{13}C$ values relative to the high $\delta^{13}C$ values of the upper North Atlantic Deep Water.

CO_3 MARs, the light values of benthic $\delta^{13}C$ in Hole 1000A (ranging between 0.4‰ and –0.3‰) occur at ~12 Ma (Episode I), ~11.4 Ma (Episode II), and ~11.0 Ma (Episode III). Light $\delta^{13}C$ values, tied to the AAIW influx within the Caribbean basins (Fig. 18B), are observed during the Holocene and last interglacial Stage 5e in the Caribbean basins, when severe carbonate dissolution occurred on the seafloor of the Caribbean basins and NADW production was at its maximum (Fig. 16).

Some of the lightest $\delta^{13}C$ values are outside of the Caribbean carbonate-crash interval, when the CO_3 MARs display some of the highest values during the middle to late Miocene transition. The intervals of 9.8–9.5 Ma (Hole 998A) and 10.0–9.5 Ma (Hole 999A) are characterized by $\delta^{13}C$ values as light as 0.1‰. We interpret the $\delta^{13}C$ fluctuations over the 2-m.y. period of the carbonate crash as driven by water mass changes. The low $\delta^{13}C$ values are tied to episodes when southern-sourced intermediate-water mass, corrosive toward carbonate sediments, fill in the Caribbean basins. Although sea-level fall at the very early part of the late Miocene may have caused the lighter $\delta^{13}C$ values observed between ~10 and 9.5 Ma, the occurrence of the lightest $\delta^{13}C$ values remains an enigma since their occurrence is not contemporaneous with poorly preserved carbonate sediments.

Global Picture

Intensification of NADW and a reorganization of the deep-water circulation would cause sedimentological changes in areas outside of the Caribbean. The link between the Caribbean carbonate crash and the re-establishment of the NADW may be better understood by observing the middle to late Miocene transition in sediments from other locations, such as the Ceara Rise (western tropical Atlantic; ODP Leg 154) and the eastern equatorial Pacific (ODP Leg 138) (Fig. 15). Evaluating how circulation changes may affect these three areas provides a way to test the effect of NADW re-establishment and intensification on the carbonate preservation in the Caribbean basins.

Leg 154 Ceara Rise: Evidence from the Equatorial Atlantic

Studies of ODP sites recovered from the Ceara Rise in the western equatorial Atlantic show that the sediments at the middle to late Miocene transition experienced similar decreases in carbonate content. Sites 925, 926, and 927 are located in water depths occupied by the NADW as determined by the data set of the Geochemical Ocean Sections Study for modern water conditions (King et al., 1997). The re-establishment and the intensification of NADW at the middle to late Miocene transition should produce conditions similar to those of the modern setting. The current overall good preservation of carbonate sediments in the area of the Ceara Rise is linked to the NADW flowing within most of the depth range of the rise and contrasts with the poor preservation of the carbonate sediments observed today in the Caribbean basins. One could expect that the preservation/dissolution pattern in the equatorial western Atlantic during the middle to late Miocene transition should be out of phase with the carbonate-preservation pattern observed in the Caribbean basins. During intervals when the NADW (or NCW) production was minimum or had ceased, such as during the early middle Miocene (Figs. 15E, 17) (Wright and Miller, 1996), the preservation of the carbonate sediment should have been minimum in the deep equatorial Atlantic Ocean and maximum in the Caribbean basins. In contrast, the opposite carbonate-preservation pattern between the deep equatorial Atlantic Ocean and the Caribbean basins should be observed at times when the NADW production was at its optimum during the late middle Miocene transition (Figs. 15E, 17) (Wright and Miller, 1996).

King et al. (1997) created synthetic records of the carbonate-content variations for the interval from 14 to 5 Ma of sites recovered from the Ceara Rise. Their results show an overall shoaling of the lysocline from 14.0 to 11.5 Ma, an interval partially predating the Caribbean carbonate crash but contemporaneous with the carbonate-crash precursor observed at Sites 999 and 1000, located south of the northern Nicaraguan Rise (Figs. 11, 12, 15). This observed lysocline shoaling contrasts with the contemporaneous overall high carbonate content and MAR in Hole 998A located on the northern side of the northern Nicaraguan Rise.

Coarse-fraction data from Site 926 on the Ceara Rise, recovered in a water depth of 3598 m, shows a smaller percentage of sand-sized material at ~13.5, 13.2–13.1, 12.6–12.4, 11.7–11.2, and 10.2–10.1 Ma (ages of Shackleton and Crowhurst, 1997, equivalent to Raffi and Flores, 1995) (Fig. 15A). Since dissolution is usually associated with a small percentage of coarse fraction and because the intervals of low proportion of coarse fraction correspond to intervals with low carbonate content, it appears that a dissolution component is recorded in the reduced carbonate content at Site 926 (Fig. 15A). At least three of the four low-carbonate intervals at 13.5, 13.1, 12.5–12.3, and 11.8 Ma (ages of Shackleton and Crowhurst, 1997), interpreted as punctuated episodes of lysocline shoaling in Hole 926A, match relatively well with intervals of relatively low values in carbonate content and accumulation rates in Hole 999A from the Colombian Basin during the carbonate-crash precursor (Fig. 15A, B). At the location of Site 926 on the Ceara Rise, the more corrosive AABW may have shoaled at times when the NADW had ceased or significantly decreased (Fig. 15E). Although some of these dissolution intervals predate the Caribbean carbonate crash and appear to be in phase with some intermediate carbonate values during the carbonate-crash precursor at Site 999, a long interval from 11.7 to 11.2 Ma characterized by very low coarse fraction and low carbonate content centered at ~11.4 Ma in Hole 926A corresponds to an interval of relatively high carbonate content and MAR at Sites 998 and 999 and is bounded by the two most intense Caribbean dissolution Episodes I and III at 12.0–11.8 and 11.1 Ma, respectively (Fig. 15).

Although the pattern of carbonate preservation between the equatorial Atlantic and the Caribbean basins during the middle and early late Miocene interval is not as clearly out of phase as the model would have predicted, it is still interesting to note that maximum carbonate dissolution occurred in the equatorial Atlantic before 11 Ma. In the middle Miocene interval prior to 12 Ma when the NADW was not fully developed (Wright and Miller, 1996), punctuated episodes of lysocline shoaling on the Ceara Rise match relatively well with intervals of carbonate dissolution in the Colombian Basin (southern Caribbean basins) during the carbonate-crash precursor and suggest that deep and intermediate waters in the equatorial Atlantic were somewhat connected and probably southern sourced and corrosive to carbonates (Fig. 15). The interval between 12 and 11 Ma, the first half of the Caribbean carbonate crash, was a transition period when the pattern of carbonate preservation became out of phase between the equatorial Atlantic and the southern and northern Caribbean basins. The two most intense episodes (I and III) of carbonate dissolution in the Caribbean basins correspond to times of good carbonate preservation in the equatorial Atlantic. Episode II, characterized by intermediate carbonate-dissolution intensity in the Caribbean basins, occurs slightly earlier than the peak dissolution at 11.4 Ma in the equatorial Atlantic. During the second half of the Caribbean carbonate-crash interval from 11 to 10 Ma, the equatorial Atlantic displays a contrasting overall good carbonate preservation. This interval is characterized in the eastern equatorial Pacific by a general decrease of the carbonate preservation, interpreted by Lyle et al. (1995) as the initial shoaling of the lysocline. (Fig. 15D)

Leg 138: Evidence from the Eastern Equatorial Pacific

When the Southern Ocean was the sole source of deep water, as in the early middle Miocene, the eastern equatorial Pacific was only half of an ocean basin away from the source. In this setting, the deep waters in the Pacific are expected to be relatively CO_2 poor and, therefore, to contain better preserved carbonate sediments. When the deep- and intermediate-water connection between the Atlantic and eastern Pacific ceased in the late middle Miocene because of the tectonic uplift of the Isthmus of Panama, the reorganization of the global thermohaline circulation, induced by the re-establishment and intensification of the NADW, located the eastern equatorial Pacific farther from the location of deep-water formation and at the end of the global conveyor belt. During times of NADW production, the establishment of a unidirectional long conveyor belt, such as the one occurring in the Holocene, would subject the eastern region of the Pacific to corrosive waters. In parallel, once deep waters are produced in the high latitudes of the Atlantic and the deep global conveyor belt is established, the Caribbean basins become the pathway for the return flow of the thermohaline circulation and are filled in with southern-sourced intermediate waters corrosive toward carbonate sediments, such as the modern AAIW. In this model and as observed at the middle to late Miocene transition, intervals of carbonate dissolution in the eastern equatorial Pacific and in the Caribbean basins are in phase.

CO_3 MARs in the Neogene sedimentary sequences recovered at ODP Leg 138 sites in the eastern equatorial Pacific (Fig. 1), as at Sites 998, 999, and 1000 in the Caribbean (Fig. 12), dramatically decrease at the middle to late Miocene transition. However, the timing of the carbonate crash in the eastern Pacific is significantly delayed when compared with the timing of the carbonate crash in the Caribbean. Although the CO_3 MAR records are only available from Hole 846B in the Peru Basin past 12.5 Ma, the CO_3 MAR reductions in several sites are centered around 11.5, 11.0–10.8, 10.5–10.3, and 10.2–10.1 Ma, and the largest, most sustained CO_3 MAR decreases occurred from 9.8 to 9.4 Ma (Figs. 1A, 15D), as well as a pronounced event at 9.0–8.8 Ma. Four of those intervals (11.5, 11.0–10.8, 10.5–10.3, and 10.2–10.1 Ma) correspond to the second, third, fourth, and fifth dissolution episodes of the Caribbean carbonate-crash intervals (Figs. 1A, 12, 15). The timing and periodicity of these four episodes of carbonate dissolution in the equatorial eastern Pacific and the Caribbean basins are identical and appear to correspond to peaks of NCW (equivalent to NADW) production (Fig. 15) (Wright and Miller, 1996). However, the high intensity of these dissolution episodes observed between 12 and 10 Ma in the Caribbean sites is only prevalent in the eastern Pacific in the interval between 11 and 9 Ma. The intensity of the carbonate crash in the eastern Pacific, therefore, lags behind by ~1 m.y. when compared with the Caribbean carbonate crash (Fig. 15). It is also curious to note and difficult to explain that the lowest CO_3 MARs in the eastern equatorial Pacific occurred at a time when the NADW production was gradually fading (Fig. 15D, F) (Wright and Miller, 1996), but seem to overlap with the Caribbean's $\delta^{13}C$ lightest values between ~10.1 and 9.5 Ma, after the Caribbean CO_3 MAR had fully recovered (Figs. 14, 15). This interval is known, as illustrated in Figures 2 and 17, to correspond to a time when the Central American Seaway was for the first time temporarily closed based upon the first recorded intermingling of large mammals between the South and North American continents (Webb, 1985) and the lack of common affinities between the Caribbean and eastern Pacific coccolith assemblages (Fig. 2B) (Kameo and Sato, in press).

It appears that the timing of the most intense dissolution interval in the eastern Pacific is linked to the temporary closure of the Central American Seaway as opposed to the global thermohaline reorganization. Not taking into account the ~1-m.y. delay between the observed maximum dissolution in the eastern equatorial Pacific relative to that in the Caribbean basins, the carbonate-dissolution episodes observed in the Caribbean and the eastern equatorial Pacific appear to be synchronous and, therefore, in phase as predicted in the model. In addition, the timing of these episodes appears to be directly linked to peaks of NADW (NCW) production, with the exception of the first NADW production peak centered at ~12 Ma, which only linked to the

first Caribbean dissolution of the carbonate crash and is conspicuously absent in the eastern Pacific CO_3 MAR records.

Figure 17 combines the summaries of Keller and Barron (1983) and Farrell et al. (1995) regarding the paleoceanographic history of the Miocene and the closure of the Isthmus of Panama, respectively. In addition, Figures 15 and 17 include new constraints based upon our analyses of the Caribbean Sites 998, 999, and 1000. Figures 15 and 17 help to place, at the middle to late Miocene transition, the occurrence of the Caribbean carbonate crash relative to the carbonate records from the equatorial Pacific and Atlantic oceans. As already suggested by Droxler et al. (1998), by triggering the subsidence of carbonate reefal barriers in the northern part of the Pedro Channel and the central region of the Walton Basin, tectonic activity in the late middle Miocene along the northern Nicaraguan Rise opened a series of new seaways to allow the establishment of the Caribbean/Loop Current system. This newly developed current system triggered an overall strengthening of the western boundary current, which transported from the Caribbean–Gulf of Mexico a large volume of saline waters, a necessary condition to explain the re-establishment and intensification of the NADW at the middle to late Miocene transition. The opening of the seaways along the northern Nicaraguan Rise, in conjunction with the uplift and partial emergence of the Isthmus of Panama, may have been crucial low-latitude controls that could explain the reorganization of global thermohaline circulation to a pattern more similar to that of today. Although other changes such as a sea-level regression or subsidence of northern North Atlantic ridges (Wright and Miller, 1996) may have played a role in the carbonate crash, the evidence from this study suggests the important factors may well have originated in the Caribbean and Central American Seaway.

CONCLUSIONS

The middle to late Miocene Caribbean carbonate crash consists of a time interval that included several massive carbonate-dissolution episodes. From 12 to 10 Ma, five distinct intervals of dissolution were recorded in the Yucatan Basin, Colombian Basin, and on the northern Nicaraguan Rise. The timing and periodicity of four of the five carbonate-dissolution episodes in the Caribbean basins appear to correspond to the peaks of NCW (equivalent to NADW) production suggested by Wright and Miller (1996) based upon the variations of the benthic $\delta^{13}C$ gradient between the North Atlantic, the southern, and eastern Pacific oceans. These findings suggest that the carbonate crash in the Caribbean was caused by a reorganization of the global thermohaline circulation induced by the re-establishment and intensification of the NADW production and concomitant influx into the Caribbean of corrosive southern-sourced intermediate waters (analogous to the modern AAIW). Because of its semi-enclosed nature below intermediate-water depths, the waters entering the Caribbean over sill depth (part of the thermohaline return flow) fill the deep Caribbean basins and affect carbonate sediment accumulation therein. At the time of the late middle Miocene carbonate crash, the Caribbean became—and remains—an important pathway for the return flow of the global thermohaline oceanic circulation.

Tectonic activity on the northern Nicaraguan Rise in the early middle Miocene led to the establishment of a connection between the southern and northern Caribbean basins by opening two new main seaways, the Pedro Channel and the Walton Basin. Once established, this connection triggered the initiation of the Caribbean Current. The gradual closing of the Central American Seaway, simultaneous to the opening of seaways along the northern Nicaraguan Rise, disrupted, temporarily shut down the low-latitude connection between the Atlantic and the eastern Pacific, and, as a direct consequence, strengthened the Caribbean Current. In the late middle Miocene, the newly developed and strengthened Caribbean Current transported warm, saline waters of the Caribbean to the northern North Atlantic via the Loop Current, the Florida Current, and the Gulf Stream. Several lines of evidence show that these different currents strengthened as the Caribbean Current was initiated.

Before the seaway opening along the northern Nicaraguan Rise, the northern Caribbean was largely isolated from the southern Caribbean basins, explaining the differences in calcareous coccolith assemblages and the absence of the Caribbean carbonate-crash precursor at Site 998 in the Yucatan Basin. At this time, well-ventilated, carbonate-rich waters entered the northern Caribbean Basin and promoted the preservation and the accumulation of carbonate sediments. In contrast, the Caribbean carbonate-crash precursor is well developed at Sites 999 and 1000, the two sites in the southern Caribbean basins. In the middle Miocene interval prior to 12 Ma when the NADW was not fully developed (Wright and Miller, 1996), the timing of several carbonate-dissolution episodes during the carbonate-crash precursor in the Colombian Basin correspond relatively well to some punctuated episodes of lysocline shoaling on the Ceara Rise. This finding suggests that the deep and intermediate waters in the equatorial Atlantic during these dissolution episodes probably had a southern source, were corrosive to carbonates, and were connected to the waters filling in the southern Caribbean basins, at least at intermediate water depths.

The re-establishment and intensification of the NADW at the middle to late Miocene transition modified the global thermohaline circulation pattern, which became comparable to that of today. The reorganization of the global oceanic circulation is well recorded in the contrasting carbonate-preservation pattern observed in the Caribbean basins, the Ceara Rise, and the eastern equatorial Pacific basins. An oxygen carbonate–rich, nutrient-poor, northern-sourced deep-water mass (NCW equivalent to the NADW) bathed the deep equatorial Atlantic (Ceara Rise) and preferentially preserved the carbonate sediments on the rise. In contrast, a southern-sourced, nutrient-rich, corrosive intermediate-water mass (similar to the modern AAIW) filled in the Caribbean basins by flowing over the sills of the Lesser Antilles and causing dissolution of the Caribbean sediments. Although the pattern of carbonate preservation between the equatorial Atlantic (Ceara Rise) and the Caribbean basins during the late middle and early late Miocene interval is not as clearly out of phase as the model would have predicted, it is still interesting to note that intervals characterized by maximum carbonate dissolution occurred in the equatorial Atlantic before 11 Ma and most of them prior to 12 Ma. The interval between 12 and 11 Ma, corresponding to the first half of the Caribbean carbonate-crash interval, was a transition period when the pattern of carbonate preservation became out of phase between the equatorial Atlantic and the southern and northern Caribbean basins. For instance, the two most intense episodes of carbonate dissolution in the Caribbean basins (Episodes I and III) correspond to times of good carbonate preservation in the deep equatorial Atlantic. During the second half of the Caribbean carbonate-crash interval, from 11 to 10 Ma, the equatorial Atlantic displays an overall pattern of good carbonate preservation and it appears to remain out of phase with the Caribbean. It is also well established that the eastern equatorial Pacific sustained considerable carbonate reductions at the middle to late Miocene transition. Intervals of intense carbonate dissolution in the eastern equatorial Pacific coincide with the younger three, possibly four, dissolution episodes of the Caribbean carbonate crash. The synchronous nature of carbonate dissolution on both sides of the Isthmus of Panama after the uplift of the isthmus to upper bathyal depths supports global causes for the carbonate crash at the middle to late Miocene transition and can be explained by the establishment of a global ocean circulation similar to the one we observe today. The postponed recovery of the carbonate system in the eastern equatorial Pacific until 9–8.5 Ma, as opposed to 10 Ma in the Caribbean basins, appears to be linked to the contemporaneous temporary complete closure of the Central American Seaway, most likely related to a major eustatic fall at ~10–9.5 Ma. Although the carbonate recovery occurred significantly earlier in the Caribbean basins than in the eastern equatorial

Pacific, the benthic $\delta^{13}C$ values in the Caribbean basins remained depleted during the nadir of the carbonate crash in the eastern equatorial Pacific. The benthic $\delta^{13}C$ records of the Caribbean basins, therefore, probably better establish the temporal and global conveyor links between the basins on either side of the Isthmus. Alternatively, the sea-level fall contemporaneous to the nadir of the carbonate crash in the eastern equatorial Pacific may be the cause for the light $\delta^{13}C$ values observed from ~10 to 9.5 Ma in the Caribbean basins rather than another pulse of NCW production. The observation that the NCW production was gradually decreasing rather than increasing during the same time interval would favor this alternative scenario.

ACKNOWLEDGMENTS

This study was supported by grants No. F000221 and F000394 from JOI/USSP/TAMRF ODP Leg 165 to André W. Droxler. We thank the crew and scientists aboard the *JOIDES Resolution* and the technical personal at the core repository in Bremen (Germany). Dennise Rodriguez and Christine Reif helped with sample preparation and analyses. Stable isotopic analyses were performed in the laboratory of Dr. Howie Spero at UC Davis. The manuscript greatly benefited from the critical comments of Dr. Mark Leckie, Dr. Mitch Lyle, Susan Swanson, and an anonymous referee. This research comprises the master's thesis of the senior author (Roth, 1998).

REFERENCES

Abreu, V.A., and Anderson, J.B., 1998. Glacial eustasy during the Cenozoic: sequence stratigraphic implications. *AAPG Bull.,* 82:1385–1400.

Barron, J.A., and Baldauf, J.G., 1989. Tertiary cooling steps and paleoproductivity as reflected by diatoms and biosiliceous sediments. *In* Berger, W.H., Smetacek, V.S., and Wefer, G. (Eds.), *Productivity of the Oceans: Present and Past:* New York (Wiley-Interscience), 341–354.

Bassinot, F.C., Beaufort, L., Vincent, E., Labeyrie, L.D., Rosteck, F., Müller, P.J., Quidelleur, X., and Lancelot, Y., 1994. Coarse fraction fluctuations in pelagic carbonate sediments from the tropical Indian Ocean: a 1,500 kyr record of carbonate dissolution. *Paleoceanography,* 9:579–600.

Belanger, P.E., Curry, W.B., and Matthews, R.K., 1981. Core-top evaluation of benthic foraminiferal isotopic ratios for paleoceanographic interpretations. *Palaeogeogr., Palaeoclimatol., Palaeoecol.,* 33:205–220.

Berger, W.H., 1970a. Biogenous deep-sea sediments: fractionation by deep-sea circulation. *Geol. Soc. Am. Bull.,* 81:1385–1401.

————, 1970b. Planktonic foraminifera: selective solution and the lysocline. *Mar. Geol.,* 8:111–138.

Berggren, W.A., Kent, D.V., Swisher, C.C., III, and Aubry, M.-P., 1995. A revised Cenozoic geochronology and chronostratigraphy. *In* Berggren, W.A., Kent, D.V., Aubry, M.-P., and Hardenbol, J. (Eds.), *Geochronology, Time Scales and Global Stratigraphic Correlation*. Spec. Publ.—Soc. Econ. Paleontol. Mineral. (Soc. Sediment. Geol.), 54:129–212.

Berggren, W.A., Kent, D.V., and Van Couvering, J.A., 1985. The Neogene, Part 2. Neogene geochronology and chronostratigraphy. *In* Snelling, N.J. (Ed.), *The Chronology of the Geological Record.* Geol. Soc. London Mem., 10:211–260.

Broecker, W.S., Bond, G., Klas, M., Bonani, G., and Wolfli, W., 1990. A salt oscillator in the glacial Atlantic? 1. The concept. *Paleoceanography,* 5:469–477.

Cande, S.C., and Kent, D.V., 1992. A new geomagnetic polarity time scale for the Late Cretaceous and Cenozoic. *J. Geophys. Res.,* 97:13917–13951.

Cunningham, A.D., 1998. The Neogene evolution of the Pedro Channel carbonate system, northern Nicaragua Rise [Ph.D. thesis]. Rice Univ., Houston.

Curry, W.B., Shackleton, N.J., Richter, C., et al., 1995. *Proc. ODP, Init. Repts.,* 154: College Station, TX (Ocean Drilling Program).

Droxler, A.W., Burke, K.C., Cunningham, A.D., Hine, A.C., Rosencrantz, E., Duncan, D.S., Hallock, P., and Robinson, E., 1998. Caribbean constraints on circulation between Atlantic and pacific Oceans over the past 40 million years. *In* Crowley, T.J., and Burke, K.C. (Eds.), *Tectonic Boundary Conditions for Climate Reconstructions:* New York (Oxford Univ. Press), 160–191.

Droxler, A.W., Cunningham, A., Hine, A.C., Hallock, P., Duncan, D., Rosencrantz, E., Buffler, R., and Robinson, E., 1992. Late middle (?) Miocene segmentation of an Eocene–early Miocene carbonate megabank on the northern Nicaragua Rise tied to the tectonic activity at the North America/Caribbean plate boundary zone. *Eos,* (Suppl. 43), 73:299.

Droxler, A.W., Morse, J.W., Glaser, K.S., Haddad, G.A., and Baker, P.A., 1991. Surface sediment carbonate mineralogy and water column chemistry: Nicaragua Rise versus the Bahamas. *Mar. Geol.,* 100:277–289.

Droxler, A.W., Morse, J.W., and Kornicker, W.A., 1988. Controls on carbonate mineral accumulation in Bahamian basins and adjacent Atlantic Ocean sediments. *J. Sediment. Petrol.,* 58:120–130.

Droxler, A.W., Schlager, W., and Whallon, C.C., 1983. Quaternary aragonite cycles and oxygen-isotope record in Bahamian carbonate ooze. *Geology,* 11:235–239.

Droxler, A.W., Staples, S.A., Rosencrantz, E., Buffler, R.T., and Baker, P.A., 1989. Neogene tectonic disintegration of a carbonate Eocene–early Miocene megabank along the Northern Nicaragua Rise, Caribbean Sea. *12th Caribbean Geol. Conf., Progr. Abstr.,* 41.

Duque-Caro, H., 1990. Major Neogene events in Panamic South America. *In* Tsuchi, R. (Ed.), *Pacific Neogene Events:* Tokyo (Univ. of Tokyo Press), 101–113.

Eberli, G.P., Wright, J.D., Bergman, K., and Anselmetti, F.S., 1998. Drift deposits at the valve of the Gulf Stream: implications for Northern Hemisphere glaciation. *Eos,* 79:F–30.

Farrell, J.W., Raffi, I., Janecek, T.C., Murray, D.W., Levitan, M., Dadey, K.A., Emeis, K.-C., Lyle, M., Flores, J.-A., and Hovan, S., 1995. Late Neogene sedimentation patterns in the eastern equatorial Pacific. *In* Pisias, N.G., Mayer, L.A., Janecek, T.R., Palmer-Julson, A., and van Andel, T.H. (Eds.), *Proc. ODP, Sci. Results,* 138: College Station, TX (Ocean Drilling Program), 717–756.

Flower, B.P., and Kennett, J. P., 1994. The middle Miocene climatic transition: East Antarctic ice sheet development, deep ocean circulation, and global carbon cycling. *Palaeogeogr., Palaeoclimatol., Palaeoecol*., 108:537–555.

Glaser, K.S., and Droxler, A.W., 1993. Controls and development of late Quaternary periplatform carbonate stratigraphy in Walton Basin (northeastern Nicaragua Rise, Caribbean Sea). *Paleoceanography,* 8: 243–274.

Gordon, A.L., 1986. Interocean exchange of thermocline water. *J. Geophys. Res.,* 91:5037–5046.

Haddad, G.A., 1994. Calcium carbonate dissolution patterns at intermediate water depths of the tropical oceans. [Ph.D. dissert.], Rice Univ., Houston.

Haddad, G.A., and Droxler, A.W., 1996. Metastable $CaCO_3$ dissolution at intermediate water depths of the Caribbean and western North Atlantic: implications for intermediate water circulation during the past 200,000 years. *Paleoceanography,* 11:701–716.

Haq, B.U., Hardenbol, J., and Vail, P.R., 1987. Chronology of fluctuating sea levels since the Triassic. *Science,* 235:1156–1167.

Kameo, K., and Sato, T., in press. Biogeography of Neogene calcareous nannofossils in the Caribbean and the eastern equatorial Pacific: floral response to the emergence of the Isthmus of Panama. *Mar. Micropaleontol.*

Keller, G., and Barron, J.A., 1983. Paleoceanographic implications of Miocene deep-sea hiatuses. *Geol. Soc. Am. Bull.,* 97:590–613.

Kennett, J.P., and Barker, P.F., 1990. Latest Cretaceous to Cenozoic climate and oceanographic developments in the Weddell Sea, Antarctica: an ocean-drilling perspective. *In* Barker, P.F., Kennett, J.P., et al., *Proc. ODP, Sci. Results,* 113: College Station, TX (Ocean Drilling Program), 937–960.

King, T.A., Ellis, W.G., Jr., Murray, D.W., Shackleton, N.J., and Harris, S., 1997. Miocene evolution of carbonate sedimentation at the Ceara Rise: a multivariate date/proxy approach. *In* Shackleton, N.J., Curry, W.B., Richter, C., and Bralower, T.J. (Eds.), *Proc. ODP, Sci. Results,* 154: College Station, TX (Ocean Drilling Program), 349–365.

Kroopnick, P., 1980. The distribution of ^{13}C in the Atlantic Ocean. *Earth Planet. Sci. Lett.,* 49:469–484.

————, 1985. The distribution of ^{13}C of ΣCO_2 in the world oceans. *Deep-Sea Res. Part A,* 32:57–84.

Le, J., Mix, A.C., and Shackleton, N.J., 1995. Late Quaternary paleoceanography in the eastern equatorial Pacific Ocean from planktonic foraminifers: a high-resolution record from Site 846. *In* Pisias, N.G., Mayer, L.A., Janecek, T.R., Palmer-Julson, A., and van Andel, T.H. (Eds.), *Proc. ODP, Sci. Results,* 138: College Station, TX (Ocean Drilling Program), 675–693.

Leroy, S., Mecier de Lepinay, B., Mauffret, A., and Pubellier, M., 1996. Structural and tectonic evolution of the eastern Cayman Trough (Caribbean Sea) from seismic reflection data. *AAPG Bull.,* 80:222–247.

Lewis, J.F., and Draper, G., 1990. Geology and tectonic evolution of the northern Caribbean margin. *In* Dengo, G., and Case, J.E. (Eds.), *The Caribbean Region.* Geol. Soc. Am., Geol. of North Am. Ser., H:77–140.

Lyle, M., Dadey, K.A., and Farrell, J.W., 1995. The late Miocene (11–8 Ma) eastern Pacific carbonate crash: evidence for reorganization of deep-water circulation by the closure of the Panama Gateway. *In* Pisias, N.G., Mayer, L.A., Janecek, T.R., Palmer-Julson, A., and van Andel, T.H. (Eds.), *Proc. ODP, Sci. Results,* 138: College Station, TX (Ocean Drilling Program), 821–838.

Maier-Reimer, E., Mikolajewicz, U., and Crowley, T., 1990. Ocean general circulation model sensitivity experiment with an open Central American isthmus. *Paleoceanography,* 5:349–366.

McDougall, K., 1985. Miocene to Pleistocene benthic foraminifers and paleoceanography of the Middle America slope, Deep Sea Drilling Project Leg 84. *In* von Huene, R., Aubouin, J., et al., *Init. Repts. DSDP,* 84: College Station, TX (Ocean Drilling Program), 363–418.

Mikolajewicz, U., and Crowley, T.J., 1997. Response of a coupled ocean/energy balance model to restricted flow through the Central American isthmus. *Paleoceanography,* 12:429–441.

Milliman, J.D., 1974. *Recent Sedimentary Carbonate:* New York (Springer-Verlag).

Müller, G., and Gastner, M., 1971. The "Karbonat-Bombe", a simple device for the determination of the carbonate content in sediments, soils and other materials. *Neues. Jahrb. Mineral. Monatsh.,* 10:466–469.

Mullins, H.T., Gardulski, A.F., Wise, S.W., Jr., and Applegate, J., 1987. Middle Miocene oceanographic event in the eastern Gulf of Mexico: implications for seismic stratigraphic succession and Loop Current/Gulf Stream circulation: *Geol. Soc. Am. Bull.,* 98:702–713.

Nishimura, S., and Suparka, S., 1997. Tectonic approach to the Neogene evolution of Pacific-Indian Ocean seaways. *Tectonophysics,* 281:1–16.

Oppo, D.W., and Fairbanks, R.G., 1990. Atlantic Ocean thermohaline circulation of the last 150,000 years: relationship to climate and atmospheric CO_2. *Paleoceanography,* 5:277–288.

Pindell, J.L., 1994. Evolution of the Gulf of Mexico and Caribbean. *In* Donovan, S., and Jackson, T.A. (Eds.), *Caribbean Geology: An Introduction:* Kingston, Jamaica (Univ. of the West Indies Publ. Assoc.), 13–39.

Pisias, N.G., Mayer, L.A., Janecek, T.R., Palmer-Julson, A., and van Andel, T.H. (Eds.), 1995. *Proc. ODP, Sci Results*, 138: College Station, TX (Ocean Drilling Program).

Popenoe, P., 1985. Cenozoic depositional and structural history of the North Carolina margin from seismic stratigraphic analyses. *In* Poag, C.W. (Ed.), *Geologic Evolution of the United States Atlantic Margin:* New York (Van Nostrand Reinhold), 125–187.

Raffi, I., and Flores, J.-A., 1995. Pleistocene through Miocene calcareous nannofossils from eastern equatorial Pacific Ocean. *In* Pisias, N.G., Mayer, L.A., Janecek, T.R., Palmer-Julson, A., and van Andel, T.H. (Eds.), *Proc. ODP, Sci. Results,* 138: College Station, TX (Ocean Drilling Program), 233–286.

Raymo, M.E., Ruddiman, W.F., Shackleton, N.J., and Oppo, D.W., 1990. Evolution of Atlantic-Pacific $\delta^{13}C$ gradients over the last 2.5 m.y. *Earth Planet. Sci. Lett.,* 97:353–368.

Roth, J.M., 1998. The Caribbean Carbonate crash at the middle to late Miocene Transition and the establishment of the modern global thermohaline circulation [M.A. thesis]. Rice Univ., Houston.

Schlager, W., Reijmer, J., and Droxler, A.W., 1994. Highstand shedding of carbonate platforms, *J. Sediment. Res.,* B64:270–281.

Schmitz, W.J., Jr., and McCartney, M.S., 1993. On the North Atlantic circulation. *Rev. Geophys.,* 31:29–49.

Schwartz, J.P., 1996. Late Quaternary periplatform sediments and paleoenvironmental analysis of Pedro Channel, northeastern Nicaraguan Rise, Caribbean Sea [M.S. thesis]. Rice Univ., Houston.

Shackleton, N.J., and Crowhurst, S., 1997. Sediment fluxes based on an orbitally tuned time scale 5 Ma to 14 Ma, Site 926. *In* Shackleton, N.J., Curry, W.B., Richter, C., and Bralower, T.J. (Eds.), *Proc. ODP, Sci. Results,* 154: College Station, TX (Ocean Drilling Program), 69–82.

Shackleton, N.J., Crowhurst, S., Hagelberg, T., Pisias, N.G., and Schneider, D.A., 1995. A new late Neogene time scale: application to Leg 138 sites. *In* Pisias, N.G., Mayer, L.A., Janecek, T.R., Palmer-Julson, A., and van Andel, T.H. (Eds.), *Proc. ODP, Sci. Results,* 138: College Station, TX (Ocean Drilling Program), 73–101.

Shackleton, N.J., and Hall, M.A., 1995. Stable isotope records in bulk sediments (Leg 138). *In* Pisias, N.G., Mayer, L.A., Janecek, T.R., Palmer-Julson, A., and van Andel, T.H. (Eds.), *Proc. ODP, Sci. Results,* 138: College Station, TX (Ocean Drilling Program), 797–805.

Shackleton, N.J., and Opdyke, N.D., 1973. Oxygen isotope and paleomagnetic stratigraphy of equatorial Pacific core V28-238: oxygen isotope temperatures and ice volumes on a 10^5 year and 10^6 year scale. *Quat. Res.,* 3:39–55.

Shearer, M.C., Peterson, L.C., Haddad, G.A., Droxler, A.W., and Carey, S.N., 1995. Deep-water Quaternary sedimentation in the Lesser Antilles Arc: detailed records of mid-depth circulation and volcanic activity. *Geol. Soc. Am. Abstr. with Progr.,* 27:A202.

Sigurdsson, H., Leckie, R.M., Acton, G.D., et al., 1997. *Proc. ODP, Init. Repts.,* 165: College Station, TX (Ocean Drilling Program).

Slowey, N.C., and Curry, W.B., 1995. Glacial-interglacial differences in circulation and carbon cycling within the upper western North Atlantic. *Paleoceanography,* 10:715–732.

Swan, A.R.H., and Sandilands, M., 1995. *Introduction to Geological Data Analysis:* Oxford (Blackwell Scientific).

Vail, P.R., and Hardenbol, J., 1979. Sea-level changes during the Tertiary. *Oceanus,* 22:71–79.

Vincent, E., 1981. Neogene carbonate stratigraphy of Hess Rise (central North Pacific) and paleoceanographic implications. *In* Thiede, J., Vallier, T.L., et al., *Init. Repts. DSDP,* 62: Washington (U.S. Govt. Printing Office), 571–606.

Vincent, E., and Berger, W.H., 1985. Carbon dioxide and polar cooling in the Miocene: the Monterey Hypothesis. *In* Sundquist, E.T., and Broecker, W.S. (Eds.), *The Carbon Cycle and Atmospheric CO_2: Natural Variations Archean to Present*. Geophys. Monogr., Am. Geophys. Union, 32:455–468.

Webb, D.S., 1985. Ecogeography and the Great American Interchange. *Paleobiology,* 17:266–280.

Wei, W., 1995. The initiation of North Atlantic Deep Water as dated by nannofossils. *J. Nannopl. Res.,* 17:90–91.

Wei, W., and Peleo-Alampay, A., 1997. Onset of North Atlantic Deep Water 11.5 million years ago triggered by climate cooling. *Proc. 30th Int. Geol. Congr. Mar. Geol. Paleoceanogr.,* 13:57–64.

Woodruff, F., and Savin, S.M., 1989. Miocene deepwater oceanography. *Paleoceanography,* 4:87–140.

Wright, J.D., and Miller, K.G., 1996. Control of the North Atlantic Deep Water. *Paleoceanography,* 11:157–170.

Wright, J.D., Miller, K.G., and Fairbanks, R.G., 1992. Miocene stable isotopes: implications for deepwater circulation and climate. *Paleoceanography,* 7:357–389.

Zachos, J.C., Flower, B.P., and Hilary, P., 1997. Orbitally paced climate oscillations across the Oligocene/Miocene boundary. *Nature,* 338:567–570.

Date of initial receipt: 25 June 1998
Date of acceptance: 21 May 1999
Ms 165SR-013